Neuronal Toll-like Receptor-4 regulation of Matrix Metalloproteinase-9 Activity Mediates Dentate Circuit Dysfunction after Traumatic Brain Injury

Deepak Subramanian[1#], Erick Contreras[1], Laura Dovek[1], Razieh Jaberi[1], Emmanuel Green[1], Ysabelle K Lao[1], Iryna M Ethell[2] and Vijayalakshmi Santhakumar[1#]

[1]Department of Molecular, Cell and Systems Biology, University of California Riverside, Riverside, California 92521, United States.

[2]Biomedical Sciences, University of California Riverside, Riverside, California 92521, United States.

Keywords: Traumatic Brain Injury, Dentate gyrus, Toll-like Receptor 4, Matrix Metalloproteinase-9, Neuro-immune signaling, Synaptic plasticity

Abstract: 287 words Full Text Character count: 75,590 Number of pages: 51

Number of figures: 7 Supplementary figures: 6 Color figures: 7

Number of tables: 0 Number of supplementary tables: 5

Correspondence:
Deepak Subramanian, PhD
Department of Molecular, Cell and Systems Biology
University of California, Riverside
E-mail: dsubra@ucr.edu

Co-Correspondence:
Vijayalakshmi Santhakumar, PhD
Department of Molecular, Cell and Systems Biology
University of California, Riverside
E-mail: vijayas@ucr.edu

List of Abbreviations:

aCSF: Artificial Cerebrospinal Fluid

AMPAR: α-Amino-3-hydroxy-5-methyl-4-isoxazolepropionic Acid Receptor

ANOVA: Analysis of Variance

CA1 SR: CA1 Stratum Radiatum

CaMKIIa: Calcium/Calmodulin-Dependent Protein Kinase II Alpha

CreERT2: Cre Recombinase Estrogen Receptor T2

DG: Dentate Gyrus

DQ Gelatinase: Dye Quenched fluorogenic substrate for zymography

ECM: Extracellular Matrix

EPSC: Excitatory Postsynaptic Current

FPI: Fluid Percussion Injury

HMGB1: High-Mobility Group Box 1

IEI: Inter-Event Interval

IPSC: Inhibitory Postsynaptic Current

JSH-23: NF-κB Inhibitor

K-S test: Kolmogorov-Smirnov Test

LPS: Lipopolysaccharide

LTP: Long Term Potentiation

MMP-9: Matrix Metalloproteinase-9

NF-κB: Nuclear Factor Kappa B

TAK-242: TLR4 Antagonist

TBS: Theta Burst Stimulation

TBI: Traumatic Brain Injury

TTX: Tetrodotoxin

Abstract:

Neuroinflammatory pathways activated by traumatic brain injury (TBI) are critical mediators of long-term neurological dysfunction and represent promising therapeutic targets. Toll-like receptor 4 (TLR4), an innate immune receptor, was previously shown to contribute to increased seizure susceptibility and cognitive deficits in rats after lateral fluid percussion injury (FPI). However, the cellular and molecular mechanisms underlying TLR4-mediated circuit dysfunction early after brain injury are not fully understood. In this study, we define a cell- and circuit- specific neuroimmune-enzyme effector signaling axis that mediates early post-TBI circuit dysfunction in the hippocampal Dentate Gyrus (DG). Using *ex vivo* electrophysiology in rat and mouse models one-week after brain injury, we demonstrate that neuronal TLR4 signaling regulates both excitatory and inhibitory synaptic inputs to dentate granule cells (DGC). Collectively, pharmacological inhibition of TLR4 in rats and cell-type-specific deletion of TLR4 in mice show that neuronal TLR4 mediates injury-driven increase in DGC excitatory input frequency and relies on downstream activation of Matrix Metalloproteinase-9 (MMP-9). In contrast, TLR4 signaling contributed to decrease in inhibitory current frequency after injury, but independent of MMP-9, revealing a mechanistic divergence. Systemic inhibition of either TLR4 signaling or MMP-9 activity in rats within 24 hours after injury reduced network hyperexcitability and improved long-term potentiation (LTP) in the DG measured *in vivo* one-week after injury. Either TLR4 or MMP-9 inhibition early after injury effectively attenuated spatial memory deficits in a Barnes maze task one-month post-injury. Paradoxically, in sham controls, inhibition of TLR4 increased frequency of both excitatory and inhibitory inputs to DGCs and augmented network

excitability, without altering MMP-9 levels, identifying context-dependent roles for TLR4 signaling. Together, these results identify a novel TLR4 -MMP-9 axis as a key driver of early post-TBI dentate gyrus circuit dysfunction and behavioral deficits.

INTRODUCTION:

Traumatic brain injury (TBI) initiates a robust and complex inflammatory cascade that exacerbates secondary structural and functional damage [1–4]. While cellular damage is widespread and diffuse, the hippocampus is highly susceptible to post-traumatic pathology. Specifically, the hippocampal dentate gyrus (DG) undergoes extensive loss of hilar neurons and circuit reorganization that critically alter hippocampal network physiology and contributes to the development of cognitive impairments and post-traumatic epilepsy [5–11]. In this context, we previously identified a pivotal role for the neuronally expressed innate immune receptor, Toll-like receptor 4 (TLR4), in enhancing neuronal excitability and driving epileptogenesis after injury [12–14]. Yet, the downstream mechanisms by which specific immune receptors influence circuit physiology remain poorly understood.

Recent evidence indicates that canonical TLR4 activators, such as lipopolysaccharide (LPS) and high-mobility group box 1 (HMGB1), can upregulate Matrix Metalloproteinase-9 (MMP-9) activity in vitro [15,16]. MMP-9 , a zinc-dependent endopeptidase, is a critical regulator of synaptic communication and plasticity through the activity-dependent degradation of the extracellular matrix (ECM)[17–20]. Importantly, MMP-9 levels are elevated early in both animal models and clinical populations after brain injury [21–24] , driving pathological remodeling of synapses and circuits that promote epileptogenesis [25–29]. Despite a strong temporal correlation between MMP-9 elevation and transient increases in TLR4 signaling after injury [12,30], a causal association between these two pathways has not been established. Based on the temporal correlation and shared

102 upstream activators, we hypothesized that mechanistic interactions between these two
103 pathways contribute to early circuit dysfunction after brain injury.

104 Here, we provide evidence for a novel mechanism involving TLR4-mediated upregulation of
105 MMP-9 activity following brain injury that drives maladaptive changes in synaptic
106 physiology, network excitability, and plasticity. Our findings reveal that the injury-induced
107 increase of MMP-9 in the dentate gyrus is specifically mediated by neuronal TLR4 signaling.
108 While TLR4-regulated MMP-9 activity was critical in enhancing excitatory synaptic inputs,
109 inhibitory input dysregulation was mediated by TLR4 signaling independent of MMP-9.
110 Furthermore, we demonstrate that this TLR4 and MMP-9 dependent pathway enhances
111 network excitability and impairs synaptic plasticity early after injury. Importantly, we show
112 that pharmacological inhibition of either TLR4 or MMP-9 effectively mitigates these early
113 pathological changes, highlighting the therapeutic potential of targeting this neuro-immune
114 signaling pathway to preserve circuit function after TBI.

115 **METHODS:**

116 All experiments were performed in accordance with IACUC protocols approved by the
117 University of California-Riverside, CA and in keeping with the ARRIVE guidelines. Male and
118 female Wistar rats (P23-P24) and mice (TLR4$^{f/f}$:CaMKIIa-CreERT2) were housed with
119 littermates in a 12-hour light/dark cycle with access to water and food ad libidum. All mice
120 were bred in-house. Animals were randomly assigned to either sham or FPI groups and
121 treatment conditions.

122 **Fluid Percussion Injury (FPI) and treatments**

123 Juvenile male and female Wistar rats (24 days old) were subjected to moderate (1.8-2.0 atm)
124 lateral FPI or sham injury using standard methods [12–14]. Briefly, a 2.7 mm hole was
125 trephined on the left side of the skull 3 mm caudal to bregma and 3.5 mm lateral from the
126 sagittal suture. A Luer-Lok syringe hub with a 3 mm inner diameter was placed over the
127 exposed dura and bonded to the skull with cyanoacrylate adhesive. The animals were
128 returned to their home cage following recovery. One day later, animals were briefly
129 anesthetized with isoflurane and attached to a fluid percussion injury device (Virginia
130 Commonwealth University, Richmond, VA, Model 01-B) directly at the metal nozzle. A
131 pendulum was dropped to deliver a brief (20ms) 1.9–2.0 atm impact on the dura. For sham
132 injury, the animals underwent surgical implantation of the hub and were anesthetized and
133 attached to the FPI device, but the pendulum was not dropped. Only rats with >10 seconds
134 apnea after injury were included in the injury group, and only the hemisphere ipsilateral to
135 the injury was examined.

136 To achieve neuron-specific deletion of TLR4, TLR4-floxed ($TLR4^{f/f}$)mice were crossed with
137 mice expressing inducible Cre recombinase under the control of the CamKIIa promoter
138 (CaMKIIa-CreERT2). Cre-positive (Cre^{+ve}) mice with TLR4 deletion and Cre-negative (Cre^{-ve})
139 littermate were used in experiments. $TLR4^{f/f}$:CaMKIIa-CreERT2 mice (8–10-week-old male
140 and female mice) were induced with tamoxifen and subjected to lateral FPI (1.5 atm) or
141 sham injury [31,32]. Tamoxifen (75mg/kg, i.p.) was prepared in 10% ethanol and 90% corn
142 oil by sonicating at 37°C for 90 minutes. Mice received 3 doses of tamoxifen, 24 hours before
143 injury, 30 minutes after injury and 24 hours after injury. TLR4 deletion in glutamatergic
144 neurons in dentate gyrus was confirmed through immunohistochemistry (see
145 immunohistochemistry methods below) and RNAscopy. Animals were treated with vehicle
146 (DMSO), TLR4 antagonist (TAK-242, 0.5mg/kg, i.p., Invivogen, San Diego, CA) or MMP-9
147 antagonist (SB-3CT, 50mg/kg, i.p., SelleckChem, Houston, TX) at 30 minutes, 8 hours, and
148 24 hours after injury. The dosing strategy for TAK-242 was based on the approach previously
149 adopted to identify functional outcomes [13,14,30,33]. Although SB3-CT has a shorter half
150 life than TAK-242 [34], prior studies have adopted 30 minutes - 24 hour dosing strategies
151 [30,33,35]. Therefore, a dosing interval similar to TAK-242 was adopted to ensure a
152 consistency in injections and animal handling across groups.

153 **Ex vivo electrophysiology**

154 One-week after FPI or sham injury, animals were anesthetized with isoflurane and
155 decapitated. Brain was quickly harvested, hemisected and coronal hippocampal slices
156 (300 µm) were prepared in ice-cold sucrose artificial cerebrospinal fluid (aCSF) containing
157 (in mM): 85 NaCl, 75 sucrose, 24 NaHCO3, 25 glucose, 4 MgCl2, 2.5 KCl, 1.25 NaH2PO4,

158 and 0.5 CaCl2 [36]. Slices were incubated at 32°C for 20 min in an interface holding chamber
159 containing an equal volume of sucrose-aCSF and recording aCSF containing (in mM) 126
160 NaCl, 2.5 KCl, 2 $CaCl_2$, 2 $MgCl_2$, 1.25 NaH_2PO_4, 26 $NaHCO_3$ and 10 D-glucose. All solutions
161 were saturated with 95% O_2 and 5% CO_2 and maintained at a pH of 7.4. Slices were allowed
162 to equilibrate for an hour at room temperature before recordings. Whole-cell voltage- and
163 current-clamp recordings were obtained from dentate granule cells (DGCs) in the
164 suprapyramidal blade at 33-34°C under IR-DIC (Olympus BX51 with 40x water immersion
165 objectives) using 3-6MΩ glass pipettes fabricated using dual stage glass micropipette puller
166 (Narishige PC-10, Amityville NY). Data was recorded using MultiClamp 700B amplifiers,
167 digitized using Digidata 1440A and acquired using pClamp10 (Molecular Devices, San Jose,
168 CA) at 10-kHz sampling frequency. Spontaneous and miniature excitatory/inhibitory
169 currents from the same DGCs were obtained using a cesium-based internal solution (in mM:
170 Cesium methanesulfonate 140, NaCl 5, HEPES 10, EGTA 0.2, Mg2ATP 2, Na2GTP 0.2, Qx314
171 5, (pH 7.25, 270-285 mOsm). Biocytin (0.2%) was included in the internal solution for post
172 hoc cell identification. Spontaneous and miniature excitatory postsynaptic potentials
173 (sEPSC and mEPSC) were recorded from the same neurons at a holding potential of -70 mV,
174 and spontaneous and miniature inhibitory postsynaptic potentials (sIPSC and mIPSC
175 respectively) were recorded at a holding potential of 0 mV. Action potential independent
176 miniature currents were isolated using tetrodotoxin (TTX, 1μM). In a subset of experiments
177 TLR4 signaling was selectively activated by incubating slices in LPS-B5 ultrapure
178 (Escherichia Coli serotype O55:B5, 10 μg/ml, Invivogen, San Diego, CA), a selective TLR4
179 agonist, for 60-90 minutes before recording [37]. Data from cell in which access resistance

180 changes over 20% during recordings and recordings with access resistance above 25 MΩ
181 were excluded from analysis. Spontaneous/miniature synaptic currents (100 events/cell)
182 were detected using template search feature in Easy Electrophysiology (version 2.6.,
183 London, UK.) by a blinded investigator and interevent intervals and amplitudes were
184 analyzed as cumulative distribution in Graphpad Prism 10.0.1 (Boston, MA).

185

186 **In vivo electrophysiology**

187 One-week after FPI/Sham injury rats were anesthetized under urethane (1.5g/kg i.p.) and
188 head-fixed onto a stereotaxic frame. Under aseptic conditions, rats were implanted with a
189 50 µm tungsten wire depth electrode (California Fine Wire company, Grover beach, CA) in
190 the granule cell layer (AP: 3-4 mm, ML: 2 mm, DV: 3-3.5 mm) guided by electrical stimulation
191 of the angular bundle (ML:4-4.2 mm, DV: 1.8-2 mm; pulse width 150µs delivered at 0.1Hz).
192 Two screw electrodes on the contralateral side served as reference and ground. The position
193 of electrodes was secured using dental cement. Acute recordings from urethane
194 anesthetized rats started 60 minutes after induction. Current-response curves were
195 obtained in response to electrical stimulation of the angular bundle (150 µs @ 0.1Hz). For
196 assessing Long Term Potentiation (LTP), DG LFP responses were evoked every 30 seconds
197 for a period of 30 minutes to establish a baseline. LTP was induced by Theta Burst Protocol
198 consisting six trains of six pulses at 400 Hz, 200 ms between trains, delivered six times at 20
199 seconds interval [38] and responses were recorded for an additional 180 minutes. At the end
200 of the experiment, animals were euthanized with a lethal dose of Euthasol (150 mg/kg, i.p.).

201 Signals were amplified 100 times (Pinnacle systems, Lawrence, KS), sampled at 10kHz,
202 digitized using PowerLab 16/35 and recorded using LabChart8 software (AD Instruments,
203 Colorado Springs, CO). Analysis was conducted using LabChart modules. Dentate spikes
204 were recorded from urethane anesthetized rats (1.5g/kg i.p.) using 16 Ch silicon probe
205 (A1x16-5mm-100-703 CM16, Neuronexus, Ann Arbor, MI). Signals were amplified 100 times
206 using Model 3600 amplifier (AM-Systems, Sequim, WA), digitized using PowerLab 16/35 and
207 recorded using Labchart8 Software (AD instruments, Colorado Springs, CO). Dentate spikes
208 were detected using Toothy analysis pipeline[39] (https://github.com/Farrell-
209 Laboratory/Toothy). Briefly, large positive events were identified using a 4.5 S.D. threshold.
210 Detected events were visually confirmed by a blinded investigator and the total number of
211 dentate spikes recorded in a 30-minute period were counted. We did not classify dentate
212 spikes as type 1 or type 2.

213 **In Situ Zymography**

214 MMP-9 activity was evaluated in hippocampal slices obtained from rats and mice 48 hours
215 after injury using a modified in situ zymography protocol [40]. Briefly, sham/injured rats or
216 TLR4$^{f/f}$:CaMKIIa-CreERT2 mice and Cre^{-ve} controls were transcardially perfused using an
217 alcohol-based formalin free tissue fixative (Accustain, A5472 Sigma-Aldrich, St.Louis, MO),
218 embedded in 2% agar and coronal slices (50μm, VF-310-0Z Compresstome, Precisionary
219 Instruments, Ashland, MA) were prepared at <4°C to preserve enzyme activity. Slices were
220 then incubated with a fluorogenic Dye Quenched gelatin substrate (1:50 dilution, Invitrogen,
221 Waltham MA) for 40 min at 37°C, washed with PBS, fixed in 4% paraformaldehyde and
222 mounted on slides in Vectashield (Vector Labs, Newark, CA). The specificity of reactions

223 was confirmed by adding MMP-9 inhibitor SB-3CT to control slices (see supplementary
224 figure 2J-K). Semiquantitative analysis of DQ fluorescence in DG molecular layer were
225 performed using ImageJ by a blinded investigator. Data was collected from 2-4 slices /
226 animals and averaged. Intensity measures were normalized to CA1 stratum radiatum since
227 we did not observe any effect of injury, treatment or genotype in this region (Supplementary
228 figure 4I-J).

229 **Single molecule fluorescent in situ hybridization (RNAscope)**

230 To visualize TLR4 in mice and MMP-9 mRNA in rat, we used RNAscope Multiplex Fluorescent
231 in situ hybridization on cryosectioned slices (20μm). RNAscope Multiplex Fluorescent
232 Reagent kit v2 assay (ACD, Newark, CA) was used following the protocol for fixed tissue [41].
233 The following kits were used for this study: RNAscope Multiplex Fluorescent Reagent kit
234 (Cat#323100), RNAscope Probe-MM-TLR4 (Cat#316801) and RNAscope probe-Rn-MMP-9
235 (Cat#532281). Slices were coverslipped with DABCO with DAPI mounting media and imaged
236 using a Zeiss Axioscope and analyzed using QuPath software by a blinded investigator.

237

238 **Immunohistochemistry**

239 Male and female TLR4$^{f/f}$:CaMKIIa-CreERT2 mice (8-10 weeks) were induced with tamoxifen
240 as described above and subjected to Sham or FPI. Three days after injury, brain tissue was
241 harvested following transcardial perfusion with PBS followed by 4% PFA. Brains were post-
242 fixed overnight and then transferred to 30% sucrose until fully equilibrated. Tissue was
243 cryosectioned at 20 μm thickness and mounted on Superfrost Plus glass slides. For

244 immunohistochemistry, slides were brought to room temperature to remove OCT and
245 washed three times in PBS. Sections were permeabilized with 0.2% Triton X-100 in PBS for
246 45 minutes at room temperature, followed by blocking with 20% goat serum for 45 minutes.
247 Sections were then incubated overnight at 4 °C with a primary antibody against TLR4 (mouse
248 anti-TLR4; Santa Cruz Biotechnology; 1:250). After three PBS washes, sections were
249 incubated with goat anti-mouse Alexa Fluor 546 secondary antibody (1:1000, Thermo Fisher,
250 S11227) for 1 hour at room temperature. Slides were washed three times with PBS and
251 mounted using an antifade mounting medium. Images were acquired using a Zeiss
252 Axioscope-5 with stereo investigator (MBF Bioscience) from three animals per group, with
253 six sections analyzed per animal. Quantification was performed using ImageJ software by
254 calculating the Corrected Total Cell Fluorescence (CTCF) in the granule cell layer and hilus
255 for each section (Supplementary figure 3 A-C).

256

257 **Stereological Estimation of Hilar Neurons**

258 To quantify neuronal loss following injury, sham and FPI rats (n = 3 and 4 rats, respectively.,
259 1-month post-injury) were deeply anesthetized with Euthasol (150 mg/kg, i.p.) and
260 transcardially perfused with PBS followed by 4% PFA. Brains were post-fixed and coronally
261 sectioned (50 μm) using a compressotome (VF-310-Z, Precisionary Instruments). Sections
262 from the side of injury were processed for Nissl staining (0.1% cresyl violet acetate and
263 0.25% glacial acetic acid). Unbiased stereological estimates of hilar neuron populations
264 were obtained using the Optical Fractionator probe (Stereo Investigator; MBF Bioscience) on

265 a Zeiss Axioscope-5 microscope by blinded investigators (See Supplementary Figure 1). Cell
266 counts from three slices were averaged within each animal and used for statistical analysis.

267 **Behavioral Experiments**

268 Rats were trained on Barnes Maze task to assess spatial learning 1-month post-injury. The
269 Barnes maze table (Maze Engineers, https://conductscience.com/maze/) was 122 cm in
270 diameter with 20 holes (10 cm each). The target hole was equipped with an escape box (22.5
271 cm x 14 cm x 9 cm LxWxH). The maze table was set up within black curtain walls with visual
272 cues and a camera installed above to record animal movement. Two bright floodlights and
273 a fan served as aversive stimuli to encourage animals reach the escape box. Animals were
274 held in their home cage outside the curtain in a dark room until their turn to run the trial. On
275 day 1, rats were habituated to the behavior room for at least 1 hour and then placed in the
276 middle of the table inside starter cup for 1 minute following which they were allowed to
277 explore the table for 180 seconds. At the end of the trial, animals were gently guided to their
278 designated escape hole. The escape hole locations were randomly assigned to each rat and
279 remained the same till the end of the experiment. The table was thoroughly wiped with
280 ethanol between tests to eliminate odor cues. Rats were subjected to a single 180-second
281 trial for 3 days. Task acquisition and retention were confirmed through tests on day 4 and
282 day 7. Four rats that fell from the table and exhibited signs of lethargy were removed from
283 the test and sacrificed. Behavioral analysis was performed by a blinded experimenter using
284 Any-maze software. Parameters such as latency to escape hole, distance travelled and
285 spatial search strategy were evaluated between sham and injured rats. Spatial search
286 strategies were scored based on 11-point scoring scheme[42]. Thigmotaxis was quantified

287 by defining a peripheral zone of the testing arena that was approximately 12 cm from the
288 outer edges of the apparatus. The proportion of time the animals spent within this
289 designated zone was recorded and used as the metric for anxiety-like behavior [43].

290

291 **Statistics**

292 Data are presented as mean ± standard error of the mean (SEM) for parametric measures,
293 or as median and interquartile range (IQR) where non-parametric distributions were
294 observed. To ensure rigorous data interpretation and minimize investigator bias, all data
295 analysis, including quantification of in situ zymography, electrophysiological recordings,
296 and behavioral scoring, was performed by researchers blinded to the treatment groups and
297 genotypes.

298 Normality of data distributions was assessed using the Shapiro-Wilk test. For the analysis
299 of synaptic events (sEPSC, mEPSC, sIPSC, and mIPSC), cumulative probability distributions
300 of inter-event intervals (IEI) and amplitudes were compared across groups using equal
301 number of consecutive events with the non-parametric Kolmogorov-Smirnov (K-S) test.
302 Effect sizes for these distributions were calculated using Cohen's d. When multiple
303 comparisons were involved (Figures 1&3, Supplementary figure 2) Holms-Bonferroni correction
304 was adopted and corrected *P* values are reported (See Supplementary table 3). Differences
305 between two groups were evaluated using two-tailed unpaired t-tests. For experiments
306 involving multiple factors, such as injury and drug treatment or injury and genotype, two-way
307 ANOVA, two-way repeated measures (RM) ANOVA (for input/output curves and behavioral

308 training days) or three-way ANOVA were employed, followed by Šídák's multiple
309 comparisons test where appropriate. Significance was defined at $P<0.05$. Statistical outlier
310 tests were not applied. Statistical analyses were performed using Graphpad Prism 10.0.1
311 (Boston, MA).

312

313

314 **RESULTS:**

315 **Neuronal TLR4 signaling is necessary for early excitatory circuit changes after brain**
316 **injury.**

317 Prior studies have identified TLR4 contribution to early changes in glutamatergic synapse
318 strength after brain injury [12–14]. However, the nature of early circuit reorganization after
319 brain injury in the dorsal hippocampus and whether immune signaling regulates these
320 changes has not been examined. Whole-cell voltage clamp recordings from DGCs in dorsal
321 hippocampal slices one-week after FPI revealed an early decrease in the inter-event
322 intervals (IEI) of spontaneous excitatory postsynaptic currents (sEPSCs), indicating an
323 increase in sEPSC frequency ($P<0.0001$ by K-S test with Holm-Šídák correction; Cohen's d
324 $= 0.34$, $n = 8$ cells/ group, Figure 1A-E, Supplementary table1 & 3). Additionally, we
325 observed a reduction in sEPSC amplitude in DGCs from rats after brain injury ($n = 8$ cells/
326 group, $P<0.0001$ by K-S test, Cohen's $d = 0.41$). To assess potential post-traumatic synaptic
327 reorganization, we recorded action potential-independent miniature EPSCs (mEPSCs) in
328 DGCs the presence of tetrodotoxin (TTX, 1 μM). Similar to sEPSCs, DGCs in rats one week
329 after FPI exhibited shorter mEPSC IEI and smaller mEPSC amplitudes compared to Sham
330 controls ($P<0.001$ by K-S test with Holm-Šídák correction; Cohen's $d = 0.22$ for IEI and 0.85
331 for amplitude, $n = 7$ cells/ group, Supplementary figure 2A-C, Supplementary table 2 & 3).
332 Together, these findings provide the first evidence of an increase in excitatory synaptic
333 inputs to DGCs in dorsal hippocampus of rats one week after injury.

334 Significant changes in synaptic inhibition are often observed early after brain injury
335 [5,7,44]. To evaluate whether inhibitory circuits are reorganized alongside the excitatory
336 circuits, we examined spontaneous inhibitory postsynaptic potentials (sIPSC) in the same
337 neurons. In contrast to changes in sEPSCs, sIPSC IEI was prolonged in DGCs from injured
338 rats (P <0.0001 by K-S test with Holm-Šídák correction; Cohen's d = 0.29, n= 8 cells/group,
339 Figure 1F-H, Supplementary tables 1 & 3). These findings indicate that in addition to
340 receiving more frequent excitatory inputs, the DGCs receive fewer inhibitory inputs after
341 brain injury. DGCs also showed an increase in sIPSC amplitude compared to sham
342 controls after brain injury (P <0.0001 by K-S test with Holm-Šídák correction; Cohen's d =
343 0.16, n = 8 cells/ group). These findings differ from our findings in the ventral hippocampus
344 demonstrating an increase in sIPSC frequency in DGCs after FPI [36,45,46]. We also
345 observed an increase in mIPSC amplitudes with no change in mIPSC IEI (Supplementary
346 Figure 2D-F, Supplementary tables 2 & 3). Together, these findings indicate an early
347 dysregulation in excitatory and inhibitory inputs to DGC's one-week after FPI. Furthermore,
348 these results identify early circuit reorganization after FPI and reveal potential differences
349 in synaptic inhibition and post-traumatic plasticity in the dorsal vs ventral hippocampus.

350 To determine whether inhibition of TLR4 signaling early after injury modified DGC synaptic
351 currents, we treated sham and FPI rats with TLR4 inhibitor TAK-242 (0.5mg/kg, i.p, 30 min, 8
352 hours and 24 hours post-injury). TAK-242 treatment reduced changes in sEPSC and mEPSC
353 frequency and amplitude in injured rats (P <0.0001 by K-S test with Holm-Šídák correction;
354 Cohen's d = 0.62 for sEPSC IEI, 0.50 for sEPSC amplitude, 0.54 for mEPSC IEI and 0.89 for
355 mEPSC amplitude, n = 8-9 cells/ group, Figure.1A-E, Supplementary figure 2A-C, and

356 Supplementary tables 1 & 3). In addition, TAK-242 reduced injury-driven changes in sIPSC
357 frequency and amplitude (*P* <0.0001 by K-S test with Holm-Šídák correction; Cohen's *d* =
358 0.22 for IEI, 0.11 for amplitude, *n* = 7-8 cells/ group, Figure.1F-H, Supplementary tables 2 &
359 3). While mIPSC frequency was unaltered, mIPSC amplitude was reduced by TAK-242
360 treatment in injured rats (*P* <0.0001 by K-S test with Holm-Šídák correction; Cohen's *d* =
361 0.47 for amplitude, *n* = 6-7 cells/ group, Supplementary figure 2D-F, Supplementary tables
362 2 & 3). These findings demonstrate a role for TLR4 signaling in driving early synaptic
363 dysregulation after FPI.

364 In contrast to injured animals, sham controls receiving TAK-242 showed paradoxically
365 opposing changes in excitatory and inhibitory synaptic inputs to DGCs. In sham controls,
366 TAK-242 treatment reduced sEPSC IEI in DGCs, increasing frequency as observed after FPI
367 but failed to alter sEPSC amplitude (*P* <0.0001 by K-S test with Holm-Šídák correction;
368 Cohen's *d* = 0.35 for IEI, *n* = 8-9 cells/ group, Figure 1B-E). Both mEPSC interval and
369 amplitude were reduced in TAK-242 treated sham controls (*P* <0.0001 by K-S test with
370 Holm-Šídák correction; Cohen's *d* = 0.24 for IEI and 0.30 for amplitude, *n* = 7-8 cells/
371 group, Supplementary figure 2A-C, Supplementary tables 2 & 3) consistent with synaptic
372 reorganization. Moreover, TAK-242 treated sham controls showed a reduction in DGC
373 sIPSC IEI and amplitude suggesting more frequent inhibitory inputs (*P* <0.01 by K-S test
374 with Holm-Šídák correction; Cohen's *d* = 0.07 for IEI and 0.21 for amplitude, *n* = 7-8 cells/
375 group, Figure 1F-H, Supplementary tables 1 & 3). However, TAK-242 treatment did not alter
376 mIPSC frequency or amplitude. Together, these findings identify a novel contribution of
377 basal TLR4 signaling in maintaining excitatory synaptic homeostasis in uninjured animals.

378 Our previous studies demonstrated neuronal TLR4 signaling as critical for post-traumatic
379 increase in DGCs AMPA currents [13]. To test whether the glutamatergic circuit changes
380 identified above require neuronal TLR4 signaling, we examined changes in sEPSC
381 frequency and amplitude in mice with selective deletion of TLR4 in CaMKII expressing
382 excitatory neurons (TLR4$^{fl/fl}$-CaMKIIa-CreERT2 mice). Care was taken to avoid constitutive
383 and developmental effects by inducing Cre recombinase just prior to injury.
384 Immunostaining for TLR4 in mice three-days after FPI, following the 3-day tamoxifen
385 induction strategy, revealed strong immunostaining for TLR4 in the granule cell layer and
386 hilus of Cre^{-ve} mice which was absent in Cre^{+ve} mice, confirming TLR4 deletion in DGCs
387 (Nested t-test: t(4) = 7.57, P = 0.0016, F(1,4) = 58.82, n = 5-6 slices from 3 mice/ group,
388 Supplementary figure 3A-C). In addition, RNAscope analysis of TLR4 mRNA confirmed the
389 lack of injury-driven TLR4 mRNA increase in Cre^{+ve} mice (F(2,9) = 8.353, P<0.05 by one-way
390 ANOVA, n = 3-5 mice/ group, Supplementary figure 3D-F). Validation studies to test for
391 effect on TLR4 deletion on neuronal intrinsic physiology failed to reveal genotype-
392 dependent effects on the resting membrane potential, input resistance or rheobase in
393 DGCs from sham controls (Supplementary figure 4C-E). However, there was a significant
394 decrease in capacitance and an increase in firing frequency in Cre^{+ve} sham mice compared
395 to Cre^{-ve} sham mice (Capacitance - Effect of Genotype- F(1,23) = 6.9, P = 0.015 by two-way
396 ANOVA; Firing frequency – Effect of Genotype – F(1,23) = 4.706, P =0.040 by three-way
397 ANOVA, n = 7 cells/ group, Supplementary figure 4B&F). Consistent with our previous
398 reports in rat and mice [31,47], there were no injury effects on DGC active properties in
399 either genotype. While there was no injury effect on DGC resting membrane potential in

400 Cre^{-ve} mice, DGCs from Cre^{+ve} mice with TLR4 deletion were more depolarized
401 (Supplementary figure 4C). Together these validation studies demonstrate the lack of
402 injury-induced TLR4 increase in Cre^{+ve} mice and suggest a role for TLR4 in basal DGC
403 excitability and maintenance of RMP after injury.

404 Having established the lack of posttraumatic TLR4 upregulation in Cre^{+ve} mice we
405 examined the contribution of neuronal TLR4 signaling to injury-induced changes in
406 synaptic inputs to DGCs. Similar to our findings in rat, brain injury reduced DGC sEPSC IEI
407 and amplitude in Cre^{-ve} mice with intact TLR4 signaling (P <0.0001 by K-S test with Holm-
408 Šídák correction; Cohen's d = 0.42 for IEI and 0.31 for amplitude, n = 7 cells/ group, Figure
409 1I-L, Supplementary table 1). Importantly, DGCs from Cre^{+ve} mice with conditional deletion
410 of TLR4 in excitatory neurons failed to exhibit injury-induced decrease in sEPSC IEI, but
411 showed a decrease in sEPSC amplitude after brain injury (P = 0.0008 by K-S test with Holm-
412 Šídák correction; Cohen's d = 0.16 for amplitude, n = 7 cells/ group. Interestingly, DGC
413 sEPSC IEI and amplitude were not different between Cre^{-ve} and Cre^{+ve} sham injured mice.
414 These findings demonstrate that TLR4 expression in glutamatergic neurons is necessary for
415 the early injury-driven changes in excitatory synaptic inputs to DGCs.

416

417 **MMP-9 activity is required for TLR4-dependent changes in DGC excitatory synapses**
418 **after brain injury**

419 We next sought to identify downstream molecular mechanisms through which TLR4
420 signaling dysregulates DGC synaptic inputs after brain injury. Several studies have reported

421 an upregulation in Matrix Metallproteinase-9 (MMP-9) expression in pre-clinical models of
422 TBI [27,30,35]. MMP-9 is a critical regulator of synaptic strength and plasticity [17,18], and
423 perturbations in MMP-9 activity is known to dysregulate synaptic physiology [19,40,48–51] .
424 Although extrinsic activation of TLR4 signaling has been shown to enhance MMP-9
425 expression in primary astrocyte/neuronal co-cultures and *in vivo* [15,16], whether TLR4
426 regulates MMP-9 activity and if this can induced synaptic and functional changes *in vivo*
427 and in the injured brain remains to be determined. Moreover, whether *neuronal* TLR4
428 regulates MMP-9 activity has not been examined.

429 To directly assess MMP-9 activity, we performed *in-situ* zymography on hippocampal slices
430 obtained from sham/FPI rats 48 hours after injury, focusing on the DG molecular layer
431 where the afferent glutamatergic synapses are located. DQ-fluorescence intensity values
432 were normalized to CA1 Stratum Radiatum (SR) since no changes were observed in this
433 region with injury, treatment or genotypes (Supplementary figure 4I-J, see methods). Our
434 experiments identified a significant increase in the MMP-9 activity in the DG molecular
435 layer in brain-injured rats compared to sham controls (MMP-activity normalized to CA1 SR:
436 Sham:14.56±2.15%, FPI:30.43±2.89%, n = 5 sham and 6 FPI rats, Figure 2A-C).
437 Pharmacologically blocking TLR4 early after FPI reduced MMP-9 activity in the DG of brain
438 injured rats ($Sham_{TAK-242}$: 17.22±2.68%, $FPI_{TAK-242}$: 16.36±2.97%, n = 5 Sham and 6 FPI rats;
439 Effect of Injury x Treatment F (1,18) = 9.13; P <0.05 by Two-way ANOVA). In contrast, MMP-9
440 activity in sham controls treated with TAK-242 was not different from vehicle treated sham
441 controls. These results identify TLR4 regulation of MMP-9 activity in the injured brain.

442 To isolate the role of neuronal TLR4 in regulating MMP-9 activity, we performed in-situ
443 zymography on mice with neuronal TLR4 deletion (TLR4$^{fl/fl}$-CaMKIIa-CreERT2) and Cre^{-ve}
444 controls (Supplementary figure 4) 48 hours after Sham or FPI. We did not observe any
445 difference in MMP-9 activity between Cre^{-ve} sham and Cre^{+ve} sham mice, indicating that
446 TLR4 deletion does not alter normal MMP-9 levels without injury (Figure 2D-F). While Cre^{-ve}
447 mice showed an increase in MMP-9 levels after injury, mice with selective TLR4 deletion in
448 glutamatergic neurons failed to develop elevated MMP-9 activity after FPI (MMP-activity
449 normalized to CA1 SR: Cre^{-ve} Sham: 13.43±3.36%, Cre^{-ve} FPI: 42.79±5.02%; Cre^{+ve} SHAM:
450 10.59±3.15%, Cre^{+ve} FPI: 12.20±1.16%., *n*=3-4 mice/group; Effect of Injury x Genotype, F
451 (1,11) = 14.70; $P<0.05$ by Two-way ANOVA, Figure 2D-F). These findings demonstrate that
452 neuronal TLR4 is necessary for the post-injury upregulation of MMP-9 activity.

453 Next, we tested the possibility that TLR4 signaling increased MMP-9 levels through
454 transcriptional upregulation. Naïve rats (P30) were injected with a selective TLR4 agonist,
455 LPS-B5 (5mg/kg., i.p.) or saline and euthanized after six hours for single molecule
456 fluorescent in situ hybridization (smFISH) to quantify MMP-9 mRNA levels. Sections from
457 LPS-B5 injected rats showed a significant increase in MMP-9 mRNA in DGCs, indicating
458 that TLR4 activation enhances MMP-9 via transcriptional upregulation (intensity A.U/μm^2:
459 saline controls 1.67±0.15; LPS-B5 treated 2.41±0.19; n= 5/group, Figure 2G-I). Furthermore,
460 inhibition of NF-κB, a key downstream effector of TLR4, using JSH-23 (10 mg/kg)
461 administered one hour before LPS-B5 injection abolished the upregulation of MMP-9
462 (intensity A.U/μm^2 : JSH-23 + LPS-B5 1.319±0.16, n = 5 rats, Main effect F(2,12) =11.20, P =
463 0.002, Figure 2G-I) Together, these findings identify TLR4 and NF-κB dependent

464 transcriptional upregulation of MMP-9 as a candidate mechanism for increase in MMP9
465 activity in the DG following brain injury.

466 MMP-9 has been shown to play a crucial role in plasticity of excitatory and inhibitory
467 synapses [52]. Therefore, we reasoned that TLR4 mediated increase in MMP-9 activity may
468 be required for the post-traumatic changes in synaptic inputs to DGCs. To examine the
469 acute effects of TLR4 signaling *ex vivo*, we compared sEPSCs in hippocampal slices from
470 sham rats incubated in LPS-B5 (10 μg/ml for 90min) or aCSF. Acute LPS-B5 incubation
471 significantly reduced sEPSC IEI in DGCs, mimicking the increase in sEPSC frequency
472 observed in FPI animals (Sham vs LPS-B5 incubated: $P < 0.0001$ by K-S test with Holm-
473 Šídák correction; Cohen's $d = 0.20$ for IEI, $n = 8$ cells from 4 rats, Figure 3A-B,C). However,
474 LPS-B5 incubation increased the sEPSC amplitude (Figure 3A-B,D). Importantly, inhibiting
475 MMP-9 using SB-3CT (10 μM) mitigated LPS-B5-induced changes in sEPSC IEI indicating
476 that TLR4-mediated alterations in excitatory synaptic inputs to DGCs require MMP-9
477 activity (LPS-B5 incubated vs SB-3CT+LPS-B5: $P < 0.0001$ by K-S test with Holm-Šídák
478 correction; Cohen's $d = 0.21$ for IEI, $n = 9$ cells from 4 rats, Figure 3A-C). Conversely, SB-
479 3CT co-incubation failed to reduce, and further exacerbated, the LPS-B5 mediated
480 increase in sEPSC amplitude (Figure 3B, D). Acute TLR4 activation failed to alter sIPSC
481 frequency but increased mIPSC interevent intervals in DGCs (Supplementary figure 5A-B).

482 Since we find that TLR4-mediated alterations in DGC sEPSC frequency requires MMP-9
483 activity, we tested if systemic inhibition of MMP-9 using SB-3CT treatment (50 mg/kg, i.p.)
484 early after FPI would prevent post-traumatic changes in excitatory inputs to DGCs. SB-3CT
485 treatment effectively mitigated injury-induced the changes in sEPSC IEI and amplitude

486 one-week after FPI in rat (*P* <0.0001 by K-S test with Holm-Šídák correction; Cohen's *d* =
487 0.60 for IEI and 0.30 for amplitude, *n* = 7 cells / group, see Supplementary table1&3, Figure
488 3E-H). Since Cre^{+ve} mice failed to show posttraumatic increase in sEPSC frequency (Figure
489 1K), we examined Cre^{-ve} mice to assess the role of MMP9 in injury-induced changes in
490 sEPSC in mice. Consistent with our findings in rat, SB-3CT treatment reduced post-injury
491 changes in sEPSC IEI in DGCs from Cre^{-ve} -negative $TLR4^{fl/fl}$-CaMKIIa-CreERT2 mice (*P*
492 <0.0001 by K-S test with Holm-Šídák correction; Cohen's *d* = 0.283 for IEI, *n* = 9 cells
493 Figure 3I-L). SB-3CT treatment did not have any effect on sIPSC frequency or amplitude
494 (Supplementary figure 5G-I) after FPI suggesting that TLR4 regulation of DGC inhibitory
495 synaptic parameters after injury does not require MMP-9 activation. However, SB-3CT
496 caused a small increase in sIPSC amplitude in sham controls (Supplementary figure 5I).
497 Together, these results indicate that injury-driven changes in excitatory, but not inhibitory,
498 inputs to DGCs required both TLR4 signaling and MMP-9 activity.

499 **Early activation of TLR4 - MMP-9 molecular axis contributes to DG network**
500 **dysfunction after brain injury**

501 Having established that the TLR4- MMP-9 mechanistic axis increases glutamatergic inputs
502 to DGCs after brain injury, we examined the contribution of this molecular pathway to early
503 changes in DG circuit function in rats *in vivo* one-week after brain injury. Input/output plots
504 of the DG population spike amplitude in response to perforant path stimulation at
505 increasing current intensities was recorded under urethane anesthesia. DG population
506 spike responses normalized to peak amplitude, revealed a leftward shift after FPI
507 indicating increased network excitability (*n* = 6 SHAM and 5 FPI rats; Effect of injury – F (1,9)

508 = 6.462, *P* = 0.031 by Two-way RM ANOVA, Figure 4A-C). This increase in network
509 excitability was mitigated by early inhibition of either TLR4 signaling or MMP-9 activity,
510 demonstrating their contribution in promoting post-traumatic DG circuit dysfunction (n= 5-
511 6 rats/group; Effect of Stimulus x Treatment: F (6,166,40.08) = 4.752, *P*=0.0009 by Two-way
512 RM ANOVA, Figure 4D). Paradoxically, as previously reported in slices [12–14], TAK-242
513 treatment increased DG population spike amplitude in sham controls (Figure 4E). However,
514 consistent with its lack of effect on EPSC frequency in sham controls, SB-3CT treatment
515 did not alter DG network excitability in sham rats (Figure 4E).

516 Enhanced network excitability combined with deficits in synaptic inhibition can increase
517 dentate throughput. We assessed DG throughput by examining dentate spikes, a distinct
518 DG population event driven by entorhinal cortex [53,54]. Linear 16- channel silicon probe
519 recordings of dentate spikes in anesthetized rats (Figure 4F-G) revealed a significant
520 increase in the frequency of dentate spikes one-week after FPI (in Hz: Sham: 0.11±0.019;
521 FPI 0.24±0.025, n = 4-5 rats/group, *P*= 0.006 by two tailed unpaired t-test), identifying
522 enhanced dentate throughput following FPI. To test if inhibition of either TLR4 signaling or
523 MMP-9 activity early after injury would reduce changes to DG throughput, we examined
524 dentate spikes in TAK-242 or SB-3CT treated sham/injured rats. Our experiments
525 demonstrate that early inhibition of either TLR4 signaling or MMP-9 activity effectively
526 prevented the post injury increase in dentate spike frequency without impacting it in sham
527 controls (n = 4-5 rats/group; Effect of Interaction F (2,21) = 9.975, *P*<0.001 by Two-way
528 ANOVA, Figure 4G).

529 We previously demonstrated that early post-injury increase in DGC calcium permeable
530 AMPA currents and deficits in working memory were mitigated by TLR4 inhibition [13]. To
531 assess whether the TLR4-MMP9 signaling impacts synaptic plasticity, we examined long-
532 term potentiation (LTP) at perforant path-DGC synapses in anesthetized rats *in vivo* using
533 theta-burst stimulation (TBS) [38]. In the first 10 minutes after TBS, the field EPSP slope
534 normalized to the maximum slope at baseline trended lower but was not statistically
535 different between sham and FPI. However, there was a reduction in the field EPSP slope at
536 60 min, 120 min, and 180 min post-TBS indicating impairment in LTP maintenance (n = 6
537 rats/group, Effect of injury : F (1,10) = 32.79, P=0.0002 by Two-way RM ANOVA with Šídák's
538 multiple comparisons 10 min: P =0.065, 60 min: P = 0.003, 120 min: P = 0.002, 180 min: P =
539 0.125, Figure 5A-E). Crucially, systemic antagonism of either TLR4 or MMP-9 early after FPI
540 effectively prevented deficits in LTP in injured rats, demonstrating contribution of TLR4-
541 MMP-9 axis to LTP deficits after brain injury (Effect of treatment: F(2,13) = 18, P=0.0002; n=
542 5-6 rats/group; See Supplementary table 4, Figure 5A-E). Consistent with the paradoxical
543 effects of TAK-242 on sEPSC and network excitability in sham controls, TAK-242 treatment
544 resulted in deficits in LTP in sham rats (Effect of treatment: F(2,13) = 8.046, P=0.0053; n= 5-
545 6 rats/group; Figure 5E). Once again, unlike TAK242, SB-3CT treatment failed to impact LTP
546 Sham rats, paralleling on the differential effects of the treatments on sEPSC frequency,
547 population spike amplitude and dentate spike frequency in sham animals. These findings
548 demonstrate that TLR4-MMP-9 dependent post-traumatic circuit changes compromise DG
549 glutamatergic circuit function and plasticity.

550 **Targeting TLR4 or MMP-9 axis early after brain injury limits long-term spatial memory**
551 **impairments.**

552 Since we identify post injury increase in dentate spikes which can compromise hippocampal
553 information processing [55–58], and blocking TLR4 and MMP-9 early after injury prevent this
554 change, we sought to determine if TLR4 and MMP-9 antagonists could alleviate long term
555 cognitive deficits after brain injury. We adopted a Barnes maze spatial learning task which
556 has been shown to rely on intact DG function[59,60]. One month after sham/FPI, brain
557 injured rats exhibited a longer latency to find the escape hole and traveled a greater total
558 distance compared to sham controls early during training but reached control levels of task
559 performance by Day 3 (See Supplementary table 5, *n* =10 rats / group, $P<0.05$ by TW-RM
560 ANOVA, Figure 6A-D). Additionally, there was no difference in task performance during trials
561 on Day 4 and Day 7, indicating that task retention is not impaired (Supplementary figure 6B-
562 C). Although there were no differences in speed of locomotion (Supplementary figure 6D),
563 injured rats showed increased thigmotaxis on Days 1 and 2 (Time spent in thigmotaxis zone
564 in seconds: $Sham_{DMSO}$ – 24.73±5.42, FPI_{DMSO} – 64.99±16.96; *n*= 10 rats/group, Effect of injury–
565 F (1,18) = 6.841, $P<0.05$ by Two-way -RM ANOVA, Figure 6I). Since injured rats showed a
566 significant increase in both thigmotaxis and latency to find the escape on Day 2 of task
567 acquisition, we examined the use of spatial strategy for navigation using a 11-point scoring
568 system [42]. Analysis of search strategies on Day 2 showed that injured animals employed
569 random or serial strategies more often, demonstrating specific deficits in ability to recall
570 spatial cues for navigation (Search strategy score_Day2: $Sham_{DMSO}$ – 7.7±0.73, FPI_{DMSO} –
571 2.4±0.47; *n*= 10 rats/group, Effect of injury– F (1,18) = 17, $P<0.01$ by Two-way RM ANOVA,

572 Figure.6E,H). These results suggest a mild delay in task acquisition after brain injury which
573 is apparent on Day 2 of the task.

574 We focused our analysis on Day 2 of task acquisition when the injury-induced impairment is
575 most apparent. Early inhibition of TLR4 signaling or MMP-9 activity prevented post-injury
576 increases in latency to escape, and distance traveled observed on Day 2 (n = 6-10 rats/group;
577 $P<0.05$ by Two-way RM ANOVA, Figure 6F-G, Supplementary table 3 and Supplementary
578 figure 6A). While the trend in ability of TLR4 inhibition to improve the strategy score in injured
579 animals did not reach statistical significance (Figure 6H), the search strategy scores in
580 injured animals significantly improved with MMP-9 inhibition (Figure 6H). Importantly, while
581 MMP-9 did not have any adverse effects on sham controls, TLR4 inhibition showed a trend
582 towards increased latency, distance travelled and thigmotaxis, and a lower spatial search
583 strategy score (Figure 6F-I) which did not reach statistical significance. Collectively, these
584 findings demonstrate that early inhibition of the TLR4-MMP-9 signaling axis effectively
585 mitigates mild long term spatial learning deficits observed after FPI.

586

587 **DISCUSSION**:

588 Understanding how immune signaling modulates neuronal function after brain injury is
589 critical for developing effective therapeutic strategies to minimize the long-term sequelae
590 of TBI. Aside from the widespread secondary injury driven by glial mediators of
591 neuroinflammation [1,2], we previously showed that the neuronal expression of innate
592 immune receptor TLR4 is upregulated in the hippocampus early after injury, contributing to

593 long-term seizure susceptibility and impaired working memory [12–14]. Here, we provide
594 mechanistic evidence that TLR4 signaling mediates rapid, circuit-level changes in both
595 excitatory and inhibitory synaptic transmission after injury. Using a combination of
596 pharmacology in rats and mouse genetics we demonstrate a central role for TLR4
597 expressed in CaMKII-positive excitatory neurons in mediating the posttraumatic circuit
598 changes through the upregulation of MMP-9. Importantly, we show that either TLR4 or
599 MMP-9 inhibition early after brain injury not only reduces these pathological changes one-
600 week after injury, but improves deficits in spatial learning 1-month after injury.

601 **TLR4 Signaling Augments Glutamatergic inputs to DGCs after brain injury.**

602 TLR4 signaling is well established as a driver of neuronal excitability [3,61–65]. Our prior
603 works showed that TLR4 signaling enhances AMPA currents in granule cells contributing to
604 DG network hyperexcitability [12,13]. Examining circuit-level changes in animals one week
605 after injury, this study identifies an aberrant increase in excitatory inputs to DGCs in the
606 dorsal hippocampus. Considering that perforant path fibers are severed in coronal
607 hippocampal slice preparations [66], the post-injury increase in spontaneous EPSCs and
608 action potential-independent miniature events observed here indicate an increase in
609 synaptic contacts, consistent with early axonal sprouting [46], or elevated mossy cell
610 excitability previously reported after FPI [67]. Our findings highlight a critical role of TLR4
611 signaling in this process. First, we show that early pharmacological inhibition of TLR4
612 mitigates changes in both spontaneous and miniature EPSC frequency. We further
613 demonstrate that transient activation of TLR4 signaling in acute brain slices using LPS-B5 is
614 sufficient to augment sEPSCs frequency to levels comparable to those seen in injured

615 animals. Furthermore, by leveraging TLR4$^{fl/fl}$: CaMKIIa-CreERT2 mice, we demonstrate that
616 selective deletion of TLR4 in glutamatergic neurons alone is sufficient to mitigate the post-
617 injury increase in sEPSC frequency. Together, these findings show that neuronal TLR4 is
618 necessary to enhance glutamatergic drive to DGCs after brain injury.

619 **A Novel Neuro-Immune-enzyme Signaling Cascade Underlies Early Post-Traumatic**
620 **Glutamatergic Circuit Plasticity**

621 To elucidate the mechanism by which TLR4 enhances glutamatergic drive to DGCs after
622 injury, we focused on MMP-9 as a potential downstream effector. MMP-9 co-localizes with
623 excitatory synapses in an activity-dependent manner, and increased MMP-9 activity is
624 known to dysregulate glutamatergic synaptic transmission [40,52,68–70]. We previously
625 reported that neuronal TLR4 enhances calcium-permeable AMPA currents in DGCs post-
626 injury by increasing the surface expression of GluA1 subunits [13]. Notably, MMP-9 activity
627 has been shown to regulate AMPA receptor mobility and synaptic accumulation of GluA1
628 subunits following chemically induced LTP [71]. In addition, TLR4 ligands such as high-
629 mobility group box 1 (HMGB1) and lipopolysaccharide (LPS) are known to enhance MMP-9
630 expression in cultures and following ischemic insult [15,16] making MMP9 an attractive
631 candidate effector of the synaptic effects of TLR4.

632 Here, we show that pharmacologically inhibiting TLR4 signaling (rats) or deleting TLR4 in
633 excitatory neurons (mice) both limit post-injury increases in MMP-9 activity identifying that
634 TLR4 signaling is necessary for injury-induced increase in MMP9. Furthermore, using LPS-
635 B5 to selectively activate TLR4, we demonstrate that activation of TLR4 is sufficient to

636 increase MMP-9 mRNA levels in the dentate gyrus of naïve rats in an NF-κB dependent
637 manner. Thus, as summarized in Figure 7, our findings identify a novel TLR4/NF-κB-
638 dependent transcriptional pathway that upregulates MMP-9 activity and promotes
639 glutamatergic circuit reorganization following brain injury. Consistent with this, inhibition of
640 MMP-9 with SB-3CT effectively reduced most of the glutamatergic circuit changes in the
641 DG resulting from direct activation of TLR4 signaling in slices (LPS-B5) and brain injury *in*
642 *vivo*.

643 **Mechanistic Divergence in TLR4 regulation of glutamatergic and GABAergic circuits**

644 In contrast to the glutamatergic inputs, we observed a decrease in the frequency of
645 inhibitory inputs to dorsal DGCs one week after FPI. This stands in direct contrast to our
646 previous findings from the ventral hippocampus [36,45,46], highlighting potential regional
647 differences in functional plasticity between dorsal and ventral hippocampal inhibitory
648 circuits [72]. While TLR4 inhibition reduced post-traumatic changes in IPSCs, this effect
649 was independent of MMP-9 activity. Although enhances MMP-9 activity is implicated in
650 hypofunction of parvalbumin expressing inhibitory neurons and perineuronal net
651 remodeling in neurodevelopmental disorders [73], we find that blocking MMP9 does not
652 impact changes in inhibitory synaptic inputs after brain injury. Notably, our findings
653 indicate a divergence of TLR4-dependent mechanisms for glutamatergic and GABAergic
654 circuit reorganization, with MMP-9-independent mechanisms contributing to changes in
655 inhibitory synapses (Figure 7). Interestingly, unlike after brain injury, selective activation of
656 TLR4 with LPS-B5 in slices from sham rats did not alter sIPSC frequency in DGCs raising the
657 possibility that injury-driven loss of hilar interneurons contributes to the reduction in sIPSC

658 after brain injury [7,47]. However, mIPSC frequency was increased following LPS-B5
659 incubation suggesting perturbations in release probability or presynaptic calcium [44,74–
660 76]. Curiously, mice with TLR4 deletion developed posttraumatic depolarization of RMP
661 not observed in cre^{-ve} controls suggesting TLR4 signaling may contribute to cell intrinsic
662 compensatory processes. Future studies should determine whether neuronal or glial TLR4
663 signaling mediates the TLR4 dependent post-injury changes in inhibition and how this
664 impacts dentate function and behaviors.

665 **Network Consequences and behavioral impact of TLR4/MMP-9 pathway.**

666 The dentate gyrus is a central node in hippocampal memory processing, regulating the flow
667 of information through the hippocampal circuit [56,77,78]. Consequently, perturbations in
668 DG circuit function can directly impact cognitive processes. Our earlier studies showed
669 enhanced perforant path evoked EPSC amplitude in DGCs after FPI, suggesting stronger
670 entorhinal-dentate coupling in the injured brain, coupled with deficits in working memory
671 [12–14]. Here we advance these findings using in vivo approaches to identify increased
672 dentate network excitability early after injury. We further show that while LTP induction was
673 unaffected after injury, LTP maintenance was compromised in injured rats. Indeed the lack
674 of deficit in LTP induction argues against a role for synaptic saturation in mediating LTP
675 deficits. Rather, we find selective deficits in LTP maintenance after brain injury indicating
676 altered transcriptional processes. Importantly, we report an increase in dentate spike
677 frequency early after brain injury indicating abnormal entorhinal-dentate throughput. Since
678 dentate spikes are critical in hippocampal information processing, memory formation, and
679 consolidation [53–57,79,80], abnormal dentate spikes could impair memory processing

680 after brain injury. Supporting this proposal, treatments that reduced dentate spike
681 frequency in injured animals also improved spatial learning deficits. Crucially, dentate
682 spikes are also increased in experimental models of epilepsy [81], suggesting that these
683 events may serve as biomarkers for post-traumatic epileptogenesis alongside the
684 pathological high frequency oscillations and altered sleep spindles identified previously
685 [82,83]. In summary, inhibition of the novel TLR4-MMP9 signaling axis after brain injury
686 preserves dentate circuit excitability and long-term potentiation while rescuing spatial
687 memory deficits (Figure 7). These results highlight the manipulation of this pathway as a
688 promising therapeutic strategy for post-traumatic recovery.

689 **A Novel Constitutive Role for TLR4 Signaling in Basal Circuit Homeostasis**

690 Our study reveals a fundamental role for basal TLR4 signaling in maintaining dentate circuit
691 homeostasis. We found that inhibition of TLR4 signaling in uninjured animals consistently
692 altered synaptic inputs, network excitability, and plasticity. Specifically, timed and
693 selective deletion of TLR4 in glutamatergic neurons in a mature circuit caused a genotype-
694 dependent reduction in granule cell capacitance and increased firing rates (Figure 7). This
695 indicates a constitutive role for neuronal TLR4 in limiting basal excitability. A reduction in
696 capacitance with increased firing in the absence of changes in action potential threshold
697 parallels observations in parvalbumin neurons in epilepsy models, where regulation of
698 perineuronal nets alters neuronal firing through effects on cell capacitance[41,84,85].
699 Indeed, our prior studies have found that ability of TLR4 blockers to increase dentate
700 excitability in uninjured controls is abolished when glial metabolic processes are
701 disrupted[14]. Our finding that TLR4 or MMP9 antagonism does not impact dentate spike

702 frequency in uninjured controls, is consistent with lack of TLR4 modulation of perforant
703 path evoked AMPA currents in the absence of injury. Nevertheless, the basal TLR4
704 regulation of network homeostasis appears critical as blocking TLR4 enhances network
705 excitability, impairs LTP maintenance and spatial memory (Figure 7). The potential for TLR4
706 inhibitors to limit the progression of epilepsy and Alzheimer's disease [11,61,86,87],
707 highlights the need to understand non-canonical TLR4 signaling in the healthy brain. Future
708 research should focus on the underlying mechanisms of basal TLR4-mediated neuronal
709 regulation.

710 Collectively, our results position the TLR4-NFkB-MMP-9 axis as a central driver of TBI-
711 induced circuit dysfunction, providing a targetable molecular pathway to serve as a
712 therapeutic target for mitigating post-traumatic epilepsy and associated cognitive deficits.

713

Declarations

Ethics approval and consent to participate

All experiments were performed in accordance with IACUC protocols approved by the University of California-Riverside, CA (Approval number #20210005/35) and in keeping with the ARRIVE guidelines.

Consent for publication

Not applicable.

Availability of data and materials

All data are available from the corresponding author upon reasonable request.

Competing interests

The authors declare no competing interests.

Funding

This work is supported by National Institutes of Health (NIH) NINDS R01 NS069861, R01NS097750 to V.S., NIH/NINDS F31NS124290 to L.D; CDMRP- Epilepsy Research Program grant W81XWH-21-1-0684 to D.S.

Authors' contributions

D.S., E.C., and L.D., performed experiments; D.S., E.C., L.D., E.G., Y.L., and R.J., analyzed data; D.S., I.E., and V.S., interpreted results of experiments; D.S. prepared figures; D.S., V.S. conception and design of research; D.S. and V.S., drafted manuscript; D.S., I.E., and V.S. finalized and approved manuscript.

Acknowledgements: We thank Dr. Leszek Kaczmarek (Nencki Institute, Warsaw, Poland) for his expert advice on *in situ* zymography. We also thank Dr. Amanda Schott and Dr. Jordan S Farrell (Harvard Medical School) for their expertise and help with Dentate spike detection algorithms.

REFERENCES:

1. Sharma R, Leung WL, Zamani A, O'brien TJ, Espinosa PMC, Semple BD. Neuroinflammation in post-traumatic epilepsy: Pathophysiology and tractable therapeutic targets. Brain Sciences. 2019 Nov 1;9(11). doi:10.3390/brainsci9110318

2. Mukherjee S, Arisi GM, Mims K, Hollingsworth G, O'Neil K, Shapiro LA. Neuroinflammatory mechanisms of post-traumatic epilepsy. Journal of Neuroinflammation. 2020 Jun 17;17(1). doi:10.1186/s12974-020-01854-w PubMed PMID: 32552898.

3. Webster KM, Sun M, Crack P, O'Brien TJ, Shultz SR, Semple BD. Inflammation in epileptogenesis after traumatic brain injury. Journal of Neuroinflammation. 2017 Jan 13;14(1). doi:10.1186/s12974-016-0786-1 PubMed PMID: 28086980.

4. Simon DW, McGeachy MJ, Baylr H, Clark RSB, Loane DJ, Kochanek PM. The far-reaching scope of neuroinflammation after traumatic brain injury. Nature Reviews Neurology. 2017 Mar 1;13(3):171–91. doi:10.1038/nrneurol.2017.13 PubMed PMID: 28186177.

5. Lowenstein D, Thomas M, Smith D, McIntosh T. Selective vulnerability of dentate hilar neurons following traumatic brain injury: a potential mechanistic link between head trauma and disorders of the hippocampus. J Neurosci. 1992 Dec 1;12(12):4846–53. doi:10.1523/JNEUROSCI.12-12-04846.1992

6. McIntosh, Saatman, Raghupathi, Graham, Smith, Lee, et al. The Dorothy Russell Memorial Lecture* The molecular and cellular sequelae of experimental traumatic brain injury: pathogenetic mechanisms. Neuropathology Appl Neurobio. 1998 Aug;24(4):251–67. doi:10.1046/j.1365-2990.1998.00121.x

7. Toth Z, Hollrigel GS, Gorcs T, Soltesz I. Instantaneous Perturbation of Dentate Interneuronal Networks by a Pressure Wave-Transient Delivered to the Neocortex. 1997.

8. Atkins CM. Decoding Hippocampal Signaling Deficits After Traumatic Brain Injury. Transl Stroke Res. 2011 Dec;2(4):546–55. doi:10.1007/s12975-011-0123-z

9. Hunt RF, Boychuk JA, Smith BN. Neural circuit mechanisms of post–traumatic epilepsy. Front Cell Neurosci. 2013;7. doi:10.3389/fncel.2013.00089

10. Paterno R, Folweiler KA, Cohen AS. Pathophysiology and Treatment of Memory Dysfunction After Traumatic Brain Injury. Curr Neurol Neurosci Rep. 2017 Jul;17(7):52. doi:10.1007/s11910-017-0762-x

11. Neuberger EJ, Gupta A, Subramanian D, Korgaonkar AA, Santhakumar V. Converging early responses to brain injury pave the road to epileptogenesis. Journal of

774 Neuroscience Research. 2019 Nov 1;97(11):1335–44. doi:10.1002/jnr.24202 PubMed
775 PMID: 29193309.

776 12. Li Y, Korgaonkar AA, Swietek B, Wang J, Elgammal FS, Elkabes S, et al. Toll-like receptor
777 4 enhancement of non-NMDA synaptic currents increases dentate excitability after
778 brain injury. Neurobiology of Disease. 2015 Feb 1;74:240–53.
779 doi:10.1016/j.nbd.2014.11.021 PubMed PMID: 25497689.

780 13. Korgaonkar AA, Li Y, Sekhar D, Subramanian D, Guevarra J, Swietek B, et al. Toll-like
781 Receptor 4 Signaling in Neurons Enhances Calcium-Permeable α-Amino-3-Hydroxy-5-
782 Methyl-4-Isoxazolepropionic Acid Receptor Currents and Drives Post-Traumatic
783 Epileptogenesis. Annals of Neurology. 2020 Apr 1;87(4):497–515.
784 doi:10.1002/ana.25698 PubMed PMID: 32031699.

785 14. Korgaonkar AA, Nguyen S, Li Y, Sekhar D, Subramanian D, Guevarra J, et al. Distinct
786 cellular mediators drive the Janus faces of toll-like receptor 4 regulation of network
787 excitability which impacts working memory performance after brain injury. Brain,
788 behavior, and immunity. 2020 Aug;88:381–95. doi:10.1016/j.bbi.2020.03.035 PubMed
789 PMID: 32259563.

790 15. Yang CC, Lin CC, Hsiao LD, Kuo JM, Tseng HC, Yang CM. Lipopolysaccharide-induced
791 matrix metalloproteinase-9 expression associated with cell migration in rat brain
792 astrocytes. International Journal of Molecular Sciences. 2020 Jan 1;21(1).
793 doi:10.3390/ijms21010259 PubMed PMID: 31905967.

794 16. Qiu J, Xu J, Zheng Y, Wei Y, Zhu X, Lo EH, et al. High-mobility group box 1 promotes
795 metalloproteinase-9 upregulation through toll-like receptor 4 after cerebral ischemia.
796 Stroke. 2010 Sep;41(9):2077–82. doi:10.1161/STROKEAHA.110.590463 PubMed PMID:
797 20671243.

798 17. Huntley GW. Synaptic circuit remodelling by matrix metalloproteinases in health and
799 disease. Nature Reviews Neuroscience. 2012 Nov;13(11):743–57.
800 doi:10.1038/nrn3320 PubMed PMID: 23047773.

801 18. Ethell IM, Ethell DW. Matrix metalloproteinases in brain development and remodeling:
802 synaptic functions and targets. Journal of neuroscience research. 2007
803 Oct;85(13):2813–23. doi:10.1002/jnr.21273 PubMed PMID: 17387691.

804 19. Szklarczyk A, Lapinska J, Rylski M, Mckay RDG, Kaczmarek L. Matrix Metalloproteinase-
805 9 Undergoes Expression and Activation during Dendritic Remodeling in Adult
806 Hippocampus. 2002.

807 20. Dityatev A, Schachner M. Extracellular matrix molecules and synaptic plasticity. Nature
808 reviews Neuroscience. 2003 Jun;4(6):456–68. doi:10.1038/nrn1115 PubMed PMID:
809 12778118.

21. Minta K, Brinkmalm G, Al Nimer F, Thelin EP, Piehl F, Tullberg M, et al. Dynamics of cerebrospinal fluid levels of matrix metalloproteinases in human traumatic brain injury. Sci Rep. 2020 Oct 22;10(1):18075. doi:10.1038/s41598-020-75233-z

22. Wang X, Jung J, Asahi M, Chwang W, Russo L, Moskowitz MA, et al. Effects of Matrix Metalloproteinase-9 Gene Knock-Out on Morphological and Motor Outcomes after Traumatic Brain Injury. 2000.

23. Hayashi T, Kaneko Y, Yu S, Bae E, Stahl CE, Kawase T, et al. Quantitative analyses of matrix metalloproteinase activity after traumatic brain injury in adult rats. Brain Research. 2009 Jul;1280:172–7. doi:10.1016/j.brainres.2009.05.040

24. Grossetete M, Phelps J, Arko L, Yonas H, Rosenberg GA. ELEVATION OF MATRIX METALLOPROTEINASES 3 AND 9 IN CEREBROSPINAL FLUID AND BLOOD IN PATIENTS WITH SEVERE TRAUMATIC BRAIN INJURY. Neurosurgery. 2009 Oct;65(4):702–8. doi:10.1227/01.NEU.0000351768.11363.48

25. Reinhard SM, Razak K, Ethell IM. A delicate balance: Role of MMP-9 in brain development and pathophysiology of neurodevelopmental disorders. Frontiers in Cellular Neuroscience. 2015 Jul 29;9(JULY). doi:10.3389/fncel.2015.00280

26. Vafadari B, Salamian A, Kaczmarek L. MMP-9 in translation: from molecule to brain physiology, pathology, and therapy. Journal of Neurochemistry. 2016 Oct 1;139:91–114. doi:10.1111/jnc.13415 PubMed PMID: 26525923.

27. Pijet B, Stefaniuk M, Kostrzewska-Ksiezyk A, Tsilibary PE, Tzinia A, Kaczmarek L. Elevation of MMP-9 Levels Promotes Epileptogenesis After Traumatic Brain Injury. Molecular Neurobiology. 2018 Dec 1;55(12):9294–306. doi:10.1007/s12035-018-1061-5 PubMed PMID: 29667129.

28. Wilczynski GM, Konopacki FA, Wilczek E, Lasiecka Z, Gorlewicz A, Michaluk P, et al. Important role of matrix metalloproteinase 9 in epileptogenesis. Journal of Cell Biology. 2008 Mar 10;180(5):1021–35. doi:10.1083/jcb.200708213 PubMed PMID: 18332222.

29. Dityatev A, Fellin T. Extracellular matrix in plasticity and epileptogenesis. Neuron Glia Biol. 2008 Aug;4(3):235–47. doi:10.1017/S1740925X09000118

30. Jia F, Pan Y hua, Mao Q, Liang Y min, Jiang J yao. Matrix metalloproteinase-9 expression and protein levels after fluid percussion injury in rats: The effect of injury severity and brain temperature. Journal of neurotrauma. 2010 Jun;27(6):1059–68. doi:10.1089/neu.2009.1067 PubMed PMID: 20233042.

31. Corrubia L, Huang A, Nguyen S, Shiflett MW, Jones MV, Ewell LA, et al. Early deficits in dentate circuit and behavioral pattern separation after concussive brain injury. Experimental Neurology. 2023 Dec;370:114578. doi:10.1016/j.expneurol.2023.114578

32. Witgen BM, Lifshitz J, Smith ML, Schwarzbach E, Liang SL, Grady MS, et al. Regional hippocampal alteration associated with cognitive deficit following experimental brain injury: A systems, network and cellular evaluation. Neuroscience. 2005;133(1):1–15. doi:10.1016/j.neuroscience.2005.01.052

33. Jia F, Yin YH, Gao GY, Wang Y, Cen L, Jiang JY. MMP-9 inhibitor SB-3CT attenuates behavioral impairments and hippocampal loss after traumatic brain injury in rat. Journal of Neurotrauma. 2014 Jul 1;31(13):1225–34. doi:10.1089/neu.2013.3230 PubMed PMID: 24661104.

34. Fumihiro J, Masaaki K, Toshiyuki T, Yoshihiko T, Takahiro K, Satoru A. Investigation of the unique metabolic fate of ethyl (6R)-6-[N-(2-chloro-4-fluorophenyl)sulfamoyl]cyclohex-1-ene-1-carboxylate (TAK-242) in rats and dogs using two types of 14C-labeled compounds having different labeled positions. Arzneimittelforschung. 2011 Nov 27;61(08):458–71. doi:10.1055/s-0031-1296228

35. Hadass O, Tomlinson BN, Gooyit M, Chen S, Purdy JJ, Walker JM, et al. Selective Inhibition of Matrix Metalloproteinase-9 Attenuates Secondary Damage Resulting from Severe Traumatic Brain Injury. PLoS ONE. 2013 Oct 23;8(10). doi:10.1371/journal.pone.0076904 PubMed PMID: 24194849.

36. Gupta A, Elgammal FS, Proddutur A, Shah S, Santhakumar V. Decrease in Tonic Inhibition Contributes to Increase in Dentate Semilunar Granule Cell Excitability after Brain Injury. J Neurosci. 2012 Feb 15;32(7):2523–37. doi:10.1523/JNEUROSCI.4141-11.2012

37. Hirschfeld M, Ma Y, Weis JH, Vogel SN, Weis JJ. Cutting edge: repurification of lipopolysaccharide eliminates signaling through both human and murine toll-like receptor 2. J Immunol. 2000 Jul 15;165(2):618–22. doi:10.4049/jimmunol.165.2.618 PubMed PMID: 10878331.

38. Cooke SF, Wu J, Plattner F, Errington M, Rowan M, Peters M, et al. Autophosphorylation of αCaMKII is not a general requirement for NMDA receptor-dependent LTP in the adult mouse. Journal of Physiology. 2006 Aug;574(3):805–18. doi:10.1113/jphysiol.2006.111559 PubMed PMID: 16728448.

39. Schott AL, Esfahany KN, Grocott JM, Farrell JS. Toothy: an interactive platform for dentate spike curation. bioRxiv. 2025 Oct 3;2025.10.03.680300. doi:10.1101/2025.10.03.680300 PubMed PMID: 41256680; PubMed Central PMCID: PMC12621741.

40. Gawlak M, Górkiewicz T, Gorlewicz A, Konopacki FA, Kaczmarek L, Wilczynski GM. High resolution in situ zymography reveals matrix metalloproteinase activity at glutamatergic synapses. Neuroscience. 2009 Jan 12;158(1):167–76. doi:10.1016/j.neuroscience.2008.05.045 PubMed PMID: 18588950.

41. Proddutur A, Nguyen S, Yeh CW, Gupta A, Santhakumar V. Reclusive chandeliers: Functional isolation of dentate axo-axonic cells after experimental status epilepticus. Progress in Neurobiology. 2023 Dec;231:102542. doi:10.1016/j.pneurobio.2023.102542

42. Rodríguez Peris L, Scheuber MI, Shan H, Braun M, Schwab ME. Barnes maze test for spatial memory: A new, sensitive scoring system for mouse search strategies. Behavioural Brain Research. 2024 Feb;458:114730. doi:10.1016/j.bbr.2023.114730

43. Harrison FE, Reiserer RS, Tomarken AJ, McDonald MP. Spatial and nonspatial escape strategies in the Barnes maze. Learn Mem. 2006 Nov;13(6):809–19. doi:10.1101/lm.334306

44. Hunt RF, Scheff SW, Smith BN. Synaptic Reorganization of Inhibitory Hilar Interneuron Circuitry after Traumatic Brain Injury in Mice. J Neurosci. 2011 May 4;31(18):6880–90. doi:10.1523/JNEUROSCI.0032-11.2011

45. Gupta A, Dovek L, Proddutur A, Elgammal FS, Santhakumar V. Long-Term Effects of Moderate Concussive Brain Injury During Adolescence on Synaptic and Tonic GABA Currents in Dentate Granule Cells and Semilunar Granule Cells. Front Neurosci. 2022;16:800733. doi:10.3389/fnins.2022.800733 PubMed PMID: 35360164; PubMed Central PMCID: PMC8964009.

46. Santhakumar V, Ratzliff ADH, Jeng J, Toth Z, Soltesz I. Long-term hyperexcitability in the hippocampus after experimental head trauma. Annals of Neurology. 2001 Dec;50(6):708–17. doi:10.1002/ana.1230

47. Santhakumar V, Bender R, Frotscher M, Ross ST, Hollrigel GS, Toth Z, et al. Granule cell hyperexcitability in the early post-traumatic rat dentate gyrus: the 'irritable mossy cell' hypothesis. The Journal of Physiology. 2000 Apr;524(1):117–34. doi:10.1111/j.1469-7793.2000.00117.x

48. Michaluk P, Wawrzyniak M, Alot P, Szczot M, Wyrembek P, Mercik K, et al. Influence of matrix metalloproteinase MMP-9 on dendritic spine morphology. J Cell Sci. 2011 Oct 1;124(Pt 19):3369–80. doi:10.1242/jcs.090852 PubMed PMID: 21896646.

49. Wiera G, Szczot M, Wojtowicz T, Lebida K, Koza P, Mozrzymas JW. Impact of matrix metalloproteinase-9 overexpression on synaptic excitatory transmission and its plasticity in rat CA3-CA1 hippocampal pathway. J Physiol Pharmacol. 2015 Apr;66(2):309–15. PubMed PMID: 25903961.

50. Nagy V, Bozdagi O, Matynia A, Balcerzyk M, Okulski P, Dzwonek J, et al. Matrix metalloproteinase-9 is required for hippocampal late-phase long-term potentiation and memory. Journal of Neuroscience. 2006 Feb 15;26(7):1923–34. doi:10.1523/JNEUROSCI.4359-05.2006 PubMed PMID: 16481424.

51. Bozdagi O, Nagy V, Kwei KT, Huntley GW. In vivo roles for matrix metalloproteinase-9 in mature hippocampal synaptic physiology and plasticity. Journal of Neurophysiology. 2007 Jul;98(1):334–44. doi:10.1152/jn.00202.2007 PubMed PMID: 17493927.

52. Wiera G, Mozrzymas JW. Extracellular Metalloproteinases in the Plasticity of Excitatory and Inhibitory Synapses. Cells. 2021 Aug 11;10(8). doi:10.3390/cells10082055 PubMed PMID: 34440823.

53. Bragin A, Jand& G, Nadasdy Z, Van Landeghem M, Buzsaki G. Dentate EEG Spikes and Associated Interneuronal Population Bursts in the Hippocampal Hilar Region of the Rat. JOURNALOF NEUROPHYSIOLOGY. 1995.

54. Penttonen M, Kamondi A, Sik A, Acsády L, Buzsáki G. Feed-forward and feed-back activation of the dentate gyrus in vivo during dentate spikes and sharp wave bursts. Hippocampus. 1997;7(4):437–50. doi:10.1002/(SICI)1098-1063(1997)7:4%3C437::AID-HIPO9%3E3.0.CO;2-F PubMed PMID: 9287083.

55. Lensu S, Waselius T, Penttonen M, Nokia MS. Dentate spikes and learning: disrupting hippocampal function during memory consolidation can improve pattern separation. J Neurophysiol. 2019;121:131–9. doi:10.1152/jn.00696.2018.-Hippocampal

56. Farrell JS, Soltesz I. Noncanonical circuits, states, and computations of the hippocampus. Science. 2025 Sep 11;389(6765):eadv4420. doi:10.1126/science.adv4420

57. Nokia MS, Gureviciene I, Waselius T, Tanila H, Penttonen M. Hippocampal electrical stimulation disrupts associative learning when targeted at dentate spikes. Journal of Physiology. 2017 Jul 15;595(14):4961–71. doi:10.1113/JP274023 PubMed PMID: 28426128.

58. Farrell JS, Hwaun E, Dudok B, Soltesz I. Neural and behavioural state switching during hippocampal dentate spikes. Nature. 2024 Apr 18;628(8008):590–5. doi:10.1038/s41586-024-07192-8

59. Bott JB, Muller MA, Jackson J, Aubert J, Cassel JC, Mathis C, et al. Spatial reference memory is associated with modulation of theta-gamma coupling in the dentate Gyrus. Cerebral Cortex. 2016 Sep 1;26(9):3744–53. doi:10.1093/cercor/bhv177 PubMed PMID: 26250776.

60. Dovek L, Ahmadi M, Marrero K, Zagha E, Santhakumar V. Cellular and circuit features distinguish dentate gyrus semilunar granule cells and granule cells activated during contextual memory formation [Internet]. 2025 Jul 17. doi:10.7554/eLife.101428.2

61. Maroso M, Balosso S, Ravizza T, Liu J, Aronica E, Iyer AM, et al. Toll-like receptor 4 and high-mobility group box-1 are involved in ictogenesis and can be targeted to reduce

954 seizures. Nature Medicine. 2010 Apr;16(4):413–9. doi:10.1038/nm.2127 PubMed
955 PMID: 20348922.

956 62. Kleen JK, Holmes GL. Taming TLR4 may ease seizures. Nature Medicine. 2010
957 Apr;16(4):369–70. doi:10.1038/nm0410-369 PubMed PMID: 20376038.

958 63. Vezzani A, Balosso S, Ravizza T. Neuroinflammatory pathways as treatment targets and
959 biomarkers in epilepsy. Nat Rev Neurol. 2019 Aug;15(8):459–72. doi:10.1038/s41582-
960 019-0217-x

961 64. Okun E, Griffioen KJ, Mattson MP. Toll-like receptor signaling in neural plasticity and
962 disease. Trends in Neurosciences. 2011 May;34(5):269–81.
963 doi:10.1016/j.tins.2011.02.005 PubMed PMID: 21419501.

964 65. Ahmad A, Crupi R, Campolo M, Genovese T, Esposito E, Cuzzocrea S. Absence of TLR4
965 Reduces Neurovascular Unit and Secondary Inflammatory Process after Traumatic
966 Brain Injury in Mice. Dhandapani KM, editor. PLoS ONE. 2013 Mar 28;8(3):e57208.
967 doi:10.1371/journal.pone.0057208

968 66. Xiong G, Metheny H, Johnson BN, Cohen AS. A comparison of different slicing planes in
969 preservation of major hippocampal pathway fibers in the mouse. Frontiers in
970 Neuroanatomy. 2017 Nov 21;11. doi:10.3389/fnana.2017.00107

971 67. Howard AL, Neu A, Morgan RJ, Echegoyen JC, Soltesz I. Opposing Modifications in
972 Intrinsic Currents and Synaptic Inputs in Post-Traumatic Mossy Cells: Evidence for
973 Single-Cell Homeostasis in a Hyperexcitable Network. Journal of Neurophysiology.
974 2007 Mar;97(3):2394–409. doi:10.1152/jn.00509.2006

975 68. Dziembowska M, Milek J, Janusz A, Rejmak E, Romanowska E, Gorkiewicz T, et al.
976 Activity-Dependent Local Translation of Matrix Metalloproteinase-9. J Neurosci. 2012
977 Oct 17;32(42):14538–47. doi:10.1523/JNEUROSCI.6028-11.2012

978 69. Dziembowska M, Wlodarczyk J. MMP9: A novel function in synaptic plasticity. The
979 International Journal of Biochemistry & Cell Biology. 2012 May;44(5):709–13.
980 doi:10.1016/j.biocel.2012.01.023

981 70. Stefaniuk M, Beroun A, Lebitko T, Markina O, Leski S, Meyza K, et al. Matrix
982 Metalloproteinase-9 and Synaptic Plasticity in the Central Amygdala in Control of
983 Alcohol-Seeking Behavior. Biological Psychiatry. 2017 Jun;81(11):907–17.
984 doi:10.1016/j.biopsych.2016.12.026

985 71. Szepesi Z, Hosy E, Ruszczycki B, Bijata M, Pyskaty M, Bikbaev A, et al. Synaptically
986 released matrix metalloproteinase activity in control of structural plasticity and the
987 cell surface distribution of GluA1-AMPA receptors. PLoS ONE. 2014 May 22;9(5).
988 doi:10.1371/journal.pone.0098274 PubMed PMID: 24853857.

72. Fanselow EE, Kubota Y, Wehr M, Yavorska I. Somatostatin-Expressing Inhibitory Interneurons in Cortical Circuits. Frontiers in Neural Circuits | www.frontiersin.org. 2016;10:76. doi:10.3389/fncir.2016.00076

73. Pirbhoy PS, Rais M, Lovelace JW, Woodard W, Razak KA, Binder DK, et al. Acute pharmacological inhibition of matrix metalloproteinase-9 activity during development restores perineuronal net formation and normalizes auditory processing in Fmr1 KO mice. Journal of Neurochemistry. 2020 Dec;155(5):538–58. doi:10.1111/jnc.15037

74. Sun DA, Deshpande LS, Sombati S, Baranova A, Wilson MS, Hamm RJ, et al. Traumatic brain injury causes a long-lasting calcium (Ca2+)-plateau of elevated intracellular Ca levels and altered Ca2+homeostatic mechanisms in hippocampal neurons surviving brain injury. Eur J of Neuroscience. 2008 Apr;27(7):1659–72. doi:10.1111/j.1460-9568.2008.06156.x

75. Weber JT. Altered Calcium Signaling Following Traumatic Brain Injury. Front Pharmacol. 2012;3. doi:10.3389/fphar.2012.00060

76. Hellstrom IC, Danik M, Luheshi GN, Williams S. Chronic LPS exposure produces changes in intrinsic membrane properties and a sustained IL-β-dependent increase in GABAergic inhibition in hippocampal CA1 pyramidal neurons. Hippocampus. 2005;15(5):656–64. doi:10.1002/hipo.20086

77. Hainmueller T, Bartos M. Dentate gyrus circuits for encoding, retrieval and discrimination of episodic memories. Nature Reviews Neuroscience. 2020 Mar 1;21(3):153–68. doi:10.1038/s41583-019-0260-z PubMed PMID: 32042144.

78. Hsu D. The dentate gyrus as a filter or gate: a look back and a look ahead. Prog Brain Res. 2007;163:601–13. doi:10.1016/S0079-6123(07)63032-5 PubMed PMID: 17765740.

79. Ewell LA. To sleep perchance to spike: a functional role for dentate spikes in memory. Journal of Physiology. 2017 Jul 15;595(14):4565. doi:10.1113/JP274502 PubMed PMID: 28485489.

80. Farrell JS, Hwaun E, Dudok B, Soltesz I. Neural and behavioural state switching during hippocampal dentate spikes [Internet]. doi:10.1038/s41586-024-07192-8

81. Flynn SP, Barrier S, Scott RC, Lenck-Santini PP, Holmes GL. Status epilepticus induced spontaneous dentate gyrus spikes: In vivo current source density analysis. PLoS ONE. 2015 Jul 6;10(7). doi:10.1371/journal.pone.0132630 PubMed PMID: 26148195.

82. Engel J, Bragin A, Staba R. Nonictal EEG biomarkers for diagnosis and treatment. Epilepsia Open. 2018 Dec 1;3(S2):120–6. doi:10.1002/epi4.12233

83. Perucca P, Smith G, Santana-Gomez C, Bragin A, Staba R. Electrophysiological biomarkers of epileptogenicity after traumatic brain injury. Neurobiology of Disease. 2019 Mar;123:69–74. doi:10.1016/j.nbd.2018.06.002

84. Tewari BP, Chaunsali L, Campbell SL, Patel DC, Goode AE, Sontheimer H. Perineuronal nets decrease membrane capacitance of peritumoral fast spiking interneurons in a model of epilepsy. Nature Communications. 2018 Dec 1;9(1). doi:10.1038/s41467-018-07113-0 PubMed PMID: 30413686.

85. Whitebirch AC, LaFrancois JJ, Jain S, Leary P, Santoro B, Siegelbaum SA, et al. Enhanced excitability of the hippocampal CA2 region and its contribution to seizure activity in a mouse model of temporal lobe epilepsy. Neuron. 2022 Oct;110(19):3121-3138.e8. doi:10.1016/j.neuron.2022.07.020

86. Zhou Y, Chen Y, Xu C, Zhang H, Lin C. TLR4 Targeting as a Promising Therapeutic Strategy for Alzheimer Disease Treatment. Front Neurosci. 2020 Dec 18;14:602508. doi:10.3389/fnins.2020.602508

87. Iori V, Iyer AM, Ravizza T, Beltrame L, Paracchini L, Marchini S, et al. Blockade of the IL-1R1/TLR4 pathway mediates disease-modification therapeutic effects in a model of acquired epilepsy. Neurobiology of Disease. 2017 Mar;99:12–23. doi:10.1016/j.nbd.2016.12.007

1043 **Figure legends:**

1044 ***Figure 1: TLR4 signaling drives early excitatory and inhibitory synaptic changes in***
1045 ***DGCs after brain injury.*** A) Schematic of the experimental question. B) Experimental
1046 timeline for examining synaptic changes after FPI in rats. C) Representative sEPSC traces
1047 showing whole-cell voltage clamp recordings from granule cells in vehicle treated sham
1048 controls (black), vehicle treated FPI (red), TLR4 inhibited sham (grey) and TLR4 inhibited FPI
1049 (blue). D-E) Cumulative probability plots of sEPSC interevent intervals (D) and amplitude
1050 (E) in vehicle treated and TLR4 inhibited sham and injured rats. F) Representative sIPSC
1051 traces showing whole-cell voltage clamp recordings from granule cells in vehicle treated
1052 sham controls (black), vehicle treated FPI (red), TLR4 inhibited sham (grey) and TLR4
1053 inhibited FPI (blue). G-H) Cumulative probability plots of sIPSC interevent intervals (G) and
1054 amplitude (H) in vehicle treated and TLR4 inhibited sham and injured rats. I) Experimental
1055 timeline for examining synaptic changes after FPI in $TLR4^{fl/fl}$: CaMKIIa- CreERT2 mice. J)
1056 Representative sEPSC traces from granule cells in Cre^{-ve} sham controls (black), Cre^{-ve} FPI
1057 (red), Cre^{+ve} sham (grey) and Cre^{+ve} FPI (blue). K-L) Cumulative probability plots of sEPSC
1058 interevent intervals (K) and amplitude (L) in granule cells from Cre^{-ve} and Cre^{+ve} mice. n = 8-9
1059 cells from 3 rats/group (A-H) and 7 cells from 3 mice/group (I-L). * indicates $P<0.05$ by K-S
1060 test with Holm-Šídák correction.

1061 ***Figure 2: TLR4 signaling upregulates MMP-9 activity in the dentate gyrus after brain***
1062 ***injury.*** A) Experimental timeline for in-situ zymography to quantify MMP-9 activity after
1063 brain injury in rat. B) Representative images showing MMP-9 activity in hippocampal
1064 sections from sham and injured rats. Images from vehicle treated (middle) and TLR

1065 inhibited mice (bottom) show MMP-9 activity in green. C) Quantification of MMP-9 activity,
1066 normalized to CA1 stratum Radiatum, shows an increase in MMP-9 activity in vehicle
1067 treated injured rats, but not in TAK-242 treated injured rats. Note that MMP-9 activity in
1068 vehicle treated and TAK-242 treated sham rats were not different. D) Experimental timeline
1069 for in-situ zymography to quantify MMP-9 activity after brain injury in mice. E)
1070 Representative images showing MMP-9 activity in sham and injured mice. Images from
1071 hippocampal sections from Cre^{-ve} sham and injured mice (top) and Cre^{+ve} sham and injured
1072 mice (bottom) show MMP-9 activity in green .F) Quantification of MMP-9 activity,
1073 normalized to CA1 stratum Radiatum, shows an increase in MMP-9 activity after brain
1074 injury in Cre^{-ve} mice, but not in Cre^{+ve} mice. Note that MMP-9 activity in sham mice was not
1075 different between genotypes. * indicates $P<0.05$, ** indicates $P<0.01$, *** indicates
1076 $P<0.001$, **** indicates $P<0.0001$ by TW-ANOVA with Šídáks multiple comparisons post
1077 hoc tests. G) Experimental timeline for RNAscope experiments in naïve rats. H)
1078 Representative images showing increase in MMP-9 mRNA in sections from rats after LPS-
1079 B5 treatment. I) Summary plot of mRNA levels in saline, LPS-B5 treated and LPS-B5+JSH-
1080 23 sections shows an increase in mRNA levels after LPS-B5 treatment which is abolished
1081 by blocking NF-κB. GCL- granule cell layer. n = 5-6 rats/group (A-C), 3-4 mice /genotype (D-
1082 F), and 5 rats/group (G-I). * indicates $P<0.05$, ** indicates $P<0.01$, by OW-ANOVA with
1083 Šídáks multiple comparisons post hoc tests. Data points in panel C, F and I represent
1084 individual animals.

1085 ***Figure 3: Blocking MMP-9 prevents early synaptic changes in excitatory inputs to DGCs***
1086 ***after brain injury.*** A) Experimental timeline for examining synaptic changes in acute rat

1087 slices after LPS incubation. B) Representative sEPSC traces from granule cells in LPS
1088 incubated (orange), LPS+SB-3CT co-incubated (magenta) slices. C-D) Cumulative
1089 probability plots of sEPSC interevent intervals (C) and amplitude (D) between LPS-B5
1090 incubated and LPS-B5+SB-3CT co-incubated slices. Note that LPS incubation significantly
1091 reduced interevent intervals. Co-incubation of slices in MMP-9 blocker SB-3CT prevented
1092 this change. E) Experimental timeline for examining synaptic changes in SB-3CT treated
1093 sham/injured rats. F) Representative granule cell sEPSC traces showing from SB-3CT
1094 treated sham (grey) and injured rats (green). G-H) Cumulative probability plots of sEPSC
1095 interevent intervals (G) and amplitude (H) in SB-3CT treated sham/injured rats. I)
1096 Experimental timeline for examining synaptic changes in SB-3CT treated Cre^{-ve} mice after
1097 brain injury. J) Representative granule cell sEPSC traces from vehicle treated (red) and SB-
1098 3CT treated mice(green). K-L) Cumulative probability plots of sEPSC interevent intervals (K)
1099 and amplitude (L) in vehicle treated and SB-3CT treated Cre^{-ve} mice. n = 8-9 cells(A-D), 7-10
1100 cells (E-H) from 3-4 rats/group and 7 cells from 3 mice /group (I-L). * indicates $P<0.05$ by K-
1101 S test with Holm-Šídák correction.

1102 ***Figure 4: TLR4 regulation of MMP-9 activity enhances dentate network excitability after***
1103 ***brain injury.*** A) Experimental timeline for *in vivo* experiments examining dentate excitability
1104 and throughput. B) Representative traces showing DG population spike from sham and
1105 injured animals in response to 800 μA stimulus (bold lines) and 1200 μA (dotted lines). C)
1106 Input-output curve illustrating early saturation of population spike amplitude in injured
1107 animals (red) compared to sham controls. D) Inhibition of TLR4 or MMP-9 effectively
1108 mitigates these changes. E) MMP-9 inhibition (light grey) did not affect input-output curves

1109 in sham animals, TLR4 inhibition increased network excitability of sham animals (grey).
1110 Sham and FPI data from panel C are included as faded traces in D (FPI) and E (Sham) for
1111 comparison. F) Representative trace from 16 channel silicon probe recording local field
1112 potentials from cortex to hippocampus. Current-source density plot shows the sink and
1113 source of an individual dentate spike. inset- a single dentate spike recorded in the GC layer.
1114 G) Quantification of dentate spikes shows a significant increase in frequency in injured
1115 animals. Inhibition of TLR4 or MMP-9 effectively reduced changes in dentate spike
1116 frequency in injured animals. n = 5-6 rats/group (A-E) and 4-5 rats/ group (F-G). *
1117 indicates<0.05, **** indicates *P*<0.0001 by TW-ANOVA with Šídáks multiple comparisons
1118 post hoc tests. Data points in panels G represent individual animals.

1119

1120 ***Figure 5: Posttraumatic deficits in long-term potentiation are improved by early***
1121 ***inhibition of TLR4 or MMP-9.*** A) Experimental timeline for *in vivo* assessment of long-term
1122 potentiation in perforant path synapses to DGCs. B) Representative traces from Sham
1123 (black) and FPI rats (red) at 10 minutes before (a) and 120 minutes after (b) LTP induction.
1124 C) Injured rats exhibit a significant decrease in fEPSP slope values after 60 minutes(red)
1125 compared to sham controls (black). D) Inhibition of TLR4 (blue) or MMP-9 (green)
1126 significantly improved LTP in injured animals. E) MMP-9 inhibition did not affect LTP in
1127 SHAM controls. TLR4 inhibition reduced LTP at 60 min and 180 min after induction. Note
1128 that Sham and FPI data from panel C are included as faded traces in D (FPI) and E (Sham)
1129 for comparison. n = 5-6 rats/group * indicates *P* <0.05 by TW-RM ANOVA.

1130 ***Figure 6: Early inhibition of TLR4 or MMP-9 improves spatial learning after brain injury.***

1131 A) Experimental timeline for testing spatial learning using Barnes maze. B) Representative

1132 heat plot showing rats trajectory during the task on day 2. C-E) Injured animals showed

1133 deficits in latency to escape, distance travelled, and search strategy on day 2. * indicates

1134 P<0.05 by RM-ANOVA. F-H) Summary plots of effect of TLR4 or MMP-9 inhibition on latency

1135 to escape (F), distance travelled (G), and search strategy (H) on day 2. I) Injured animals

1136 showed increased thigmotaxis on day 2 which was attenuated with TLR4 or MMP-9

1137 inhibition. n = 6-10 rats/group. * indicates P<0.05, ** indicates *P*<0.01, *** indicates

1138 *P*<0.001, **** indicates *P*<0.0001 by TW-ANOVA with Šídáks multiple comparisons post

1139 hoc tests. Data points in panels F-I represent individual animals.

1140

1141

1142 ***Figure 7: Graphical Summary of TLR4 regulation of dentate gyrus function in control***

1143 ***and injured brain.***

1144 In uninjured brain, pharmacological inhibition of TLR4 signaling increases the frequency of

1145 both excitatory and inhibitory currents and enhances network excitability and impairs long-

1146 term potentiation without altering MMP-9 activity. Genetic deletion of neuronal TLR4 alters

1147 intrinsic properties without impacting synaptic physiology. Together these data are

1148 consistent with non-neuronal TLR4 signaling contributing to basal synaptic homeostasis in

1149 line with prior ex vivo studies [14]. In the injured brain, augmented neuronal TLR4 signaling

1150 acts through MMP-9 to enhance glutamatergic signaling, network excitability and dentate

1151 spikes and impairs LTP maintenance. Mechanistically, inhibitory changes are driven by

1152 TLR4 in an MMP-9 independent manner. Together, these findings demonstrate that TLR4

1153 signaling regulates DG function and seizure susceptibility [13] through distinct, context-

1154 dependent cellular mechanisms in the healthy and injured brain.† refers to [14] ‡ refers to

1155 [13].

1156

1157

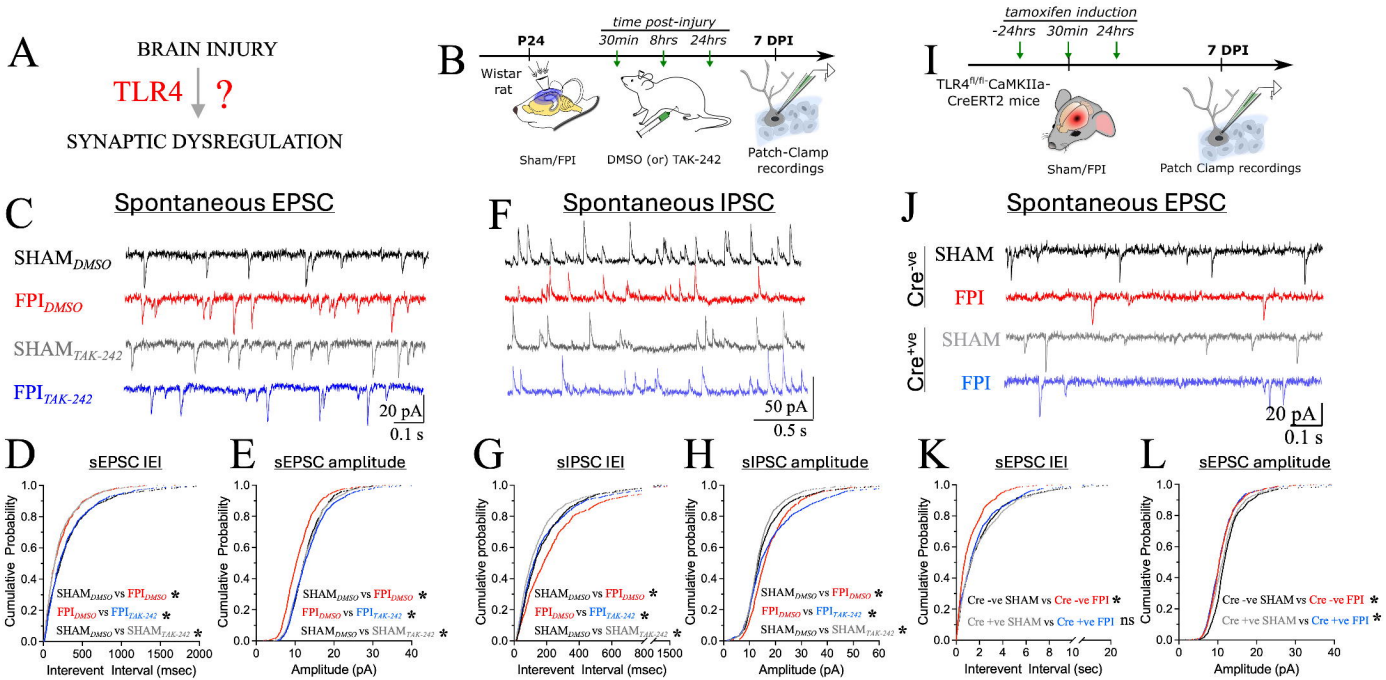
A
BRAIN INJURY
TLR4 ?
SYNAPTIC DYSREGULATION
B
time post-injury
P24
30min 8hrs 24hrs
7 DPI
Wistar rat
Sham/FPI
DMSO (or) TAK-242
Patch-Clamp recordings
I
tamoxifen induction
-24hrs 30min 24hrs
7 DPI
TLR4fl/fl-CaMKIIa-CreERT2 mice
Sham/FPI
Patch Clamp recordings
C
Spontaneous EPSC
SHAMDMSO
FPIDMSO
SHAMTAK-242
FPITAK-242
20 pA
0.1 s
F
Spontaneous IPSC
50 pA
0.5 s
J
Spontaneous EPSC
Cre-ve
SHAM
FPI
Cre+ve
SHAM
FPI
20 pA
0.1 s
D
sEPSC IEI
Cumulative Probability
SHAMDMSO vs FPIDMSO *
FPIDMSO vs FPITAK-242 *
SHAMDMSO vs SHAMTAK-242 *
Interevent Interval (msec)
E
sEPSC amplitude
Cumulative Probability
SHAMDMSO vs FPIDMSO *
FPIDMSO vs FPITAK-242 *
SHAMDMSO vs SHAMTAK-242 *
Amplitude (pA)
G
sIPSC IEI
Cumulative probability
SHAMDMSO vs FPIDMSO *
FPIDMSO vs FPITAK-242 *
SHAMDMSO vs SHAMTAK-242 *
Interevent Interval (msec)
H
sIPSC amplitude
Cumulative probability
SHAMDMSO vs FPIDMSO *
FPIDMSO vs FPITAK-242 *
SHAMDMSO vs SHAMTAK-242 *
Amplitude (pA)
K
sEPSC IEI
Cumulative Probability
Cre -ve SHAM vs Cre -ve FPI *
Cre +ve SHAM vs Cre +ve FPI ns
Interevent Interval (sec)
L
sEPSC amplitude
Cumulative Probability
Cre -ve SHAM vs Cre -ve FPI *
Cre +ve SHAM vs Cre +ve FPI *
Amplitude (pA)

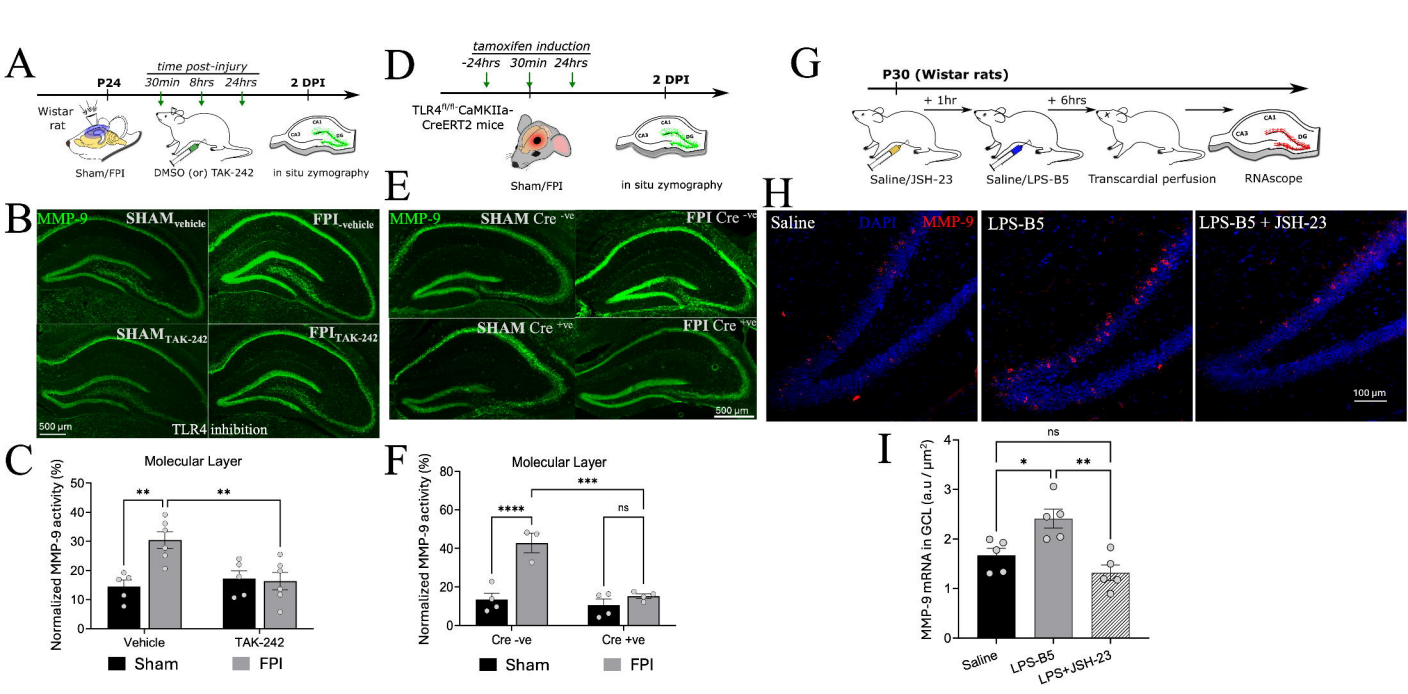
A
time post-injury
P24
30min
8hrs
24hrs
2 DPI
Wistar rat
Sham/FPI
DMSO (or) TAK-242
in situ zymography
D
tamoxifen induction
-24hrs
30min
24hrs
2 DPI
TLR4fl/fl CaMKIIa-CreERT2 mice
Sham/FPI
in situ zymography
G
P30 (Wistar rats)
+ 1hr
+ 6hrs
Saline/JSH-23
Saline/LPS-B5
Transcardial perfusion
RNAscope
B
MMP-9
SHAMvehicle
FPIvehicle
SHAMTAK-242
FPITAK-242
500 µm
TLR4 inhibition
E
MMP-9
SHAM Cre -ve
FPI Cre -ve
SHAM Cre +ve
FPI Cre +ve
500 µm
H
Saline
DAPI
MMP-9
LPS-B5
LPS-B5 + JSH-23
100 µm
C
Molecular Layer
Normalized MMP-9 activity (%)
Vehicle
TAK-242
Sham
FPI
F
Molecular Layer
Normalized MMP-9 activity (%)
Cre -ve
Cre +ve
Sham
FPI
I
MMP-9 mRNA in GCL (a.u / µm²)
Saline
LPS-B5
LPS+JSH-23

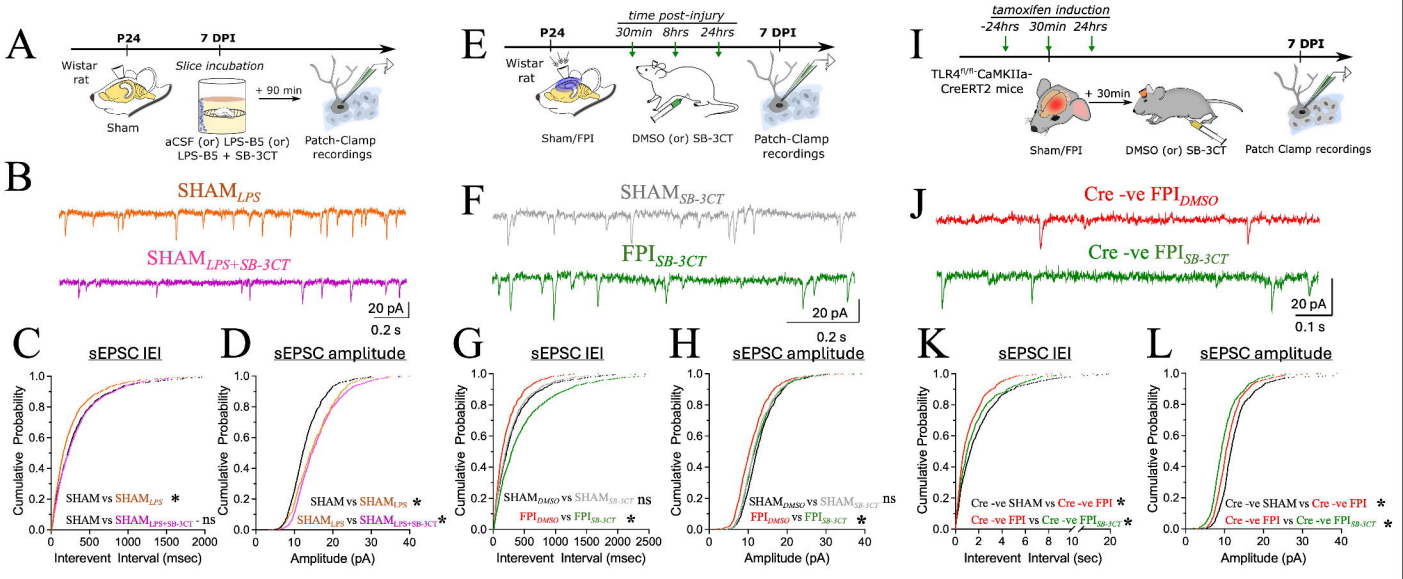
A
P24
7 DPI
Wistar rat
Slice incubation
+ 90 min
Sham
aCSF (or) LPS-B5 (or) LPS-B5 + SB-3CT
Patch-Clamp recordings
E
time post-injury
30min 8hrs 24hrs
P24
7 DPI
Wistar rat
Sham/FPI
DMSO (or) SB-3CT
Patch-Clamp recordings
I
tamoxifen induction
-24hrs 30min 24hrs
7 DPI
TLR4fl/fl-CaMKIIa-CreERT2 mice
+ 30min
Sham/FPI
DMSO (or) SB-3CT
Patch Clamp recordings
B
SHAMLPS
SHAMLPS+SB-3CT
20 pA
0.2 s
F
SHAMSB-3CT
FPISB-3CT
20 pA
0.2 s
J
Cre -ve FPIDMSO
Cre -ve FPISB-3CT
20 pA
0.1 s
C
sEPSC IEI
Cumulative Probability
SHAM vs SHAMLPS *
SHAM vs SHAMLPS+SB-3CT - ns
Interevent Interval (msec)
D
sEPSC amplitude
SHAM vs SHAMLPS *
SHAMLPS vs SHAMLPS+SB-3CT *
Amplitude (pA)
G
sEPSC IEI
SHAMDMSO vs SHAMSB-3CT ns
FPIDMSO vs FPISB-3CT *
Interevent Interval (msec)
H
sEPSC amplitude
SHAMDMSO vs SHAMSB-3CT ns
FPIDMSO vs FPISB-3CT *
Amplitude (pA)
K
sEPSC IEI
Cre -ve SHAM vs Cre -ve FPI *
Cre -ve FPI vs Cre -ve FPISB-3CT *
Interevent Interval (sec)
L
sEPSC amplitude
Cre -ve SHAM vs Cre -ve FPI *
Cre -ve FPI vs Cre -ve FPISB-3CT *
Amplitude (pA)

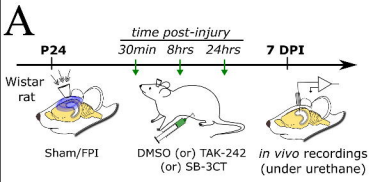
A
time post-injury
P24
30min
8hrs
24hrs
7 DPI
Wistar rat
Sham/FPI
DMSO (or) TAK-242 (or) SB-3CT
in vivo recordings (under urethane)

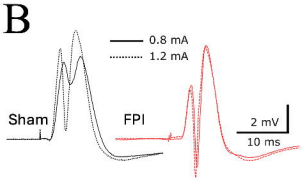
B
0.8 mA
1.2 mA
Sham
FPI
2 mV
10 ms

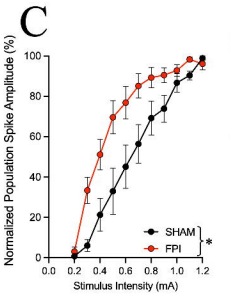
C
Normalized Population Spike Amplitude (%)
Stimulus Intensity (mA)
SHAM
FPI
*

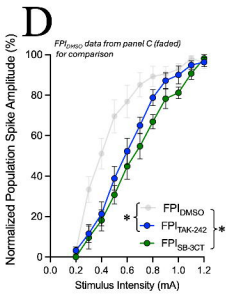
D
FPI DMSO data from panel C (faded) for comparison
Normalized Population Spike Amplitude (%)
Stimulus Intensity (mA)
FPI DMSO
FPI TAK-242
FPI SB-3CT
*
*

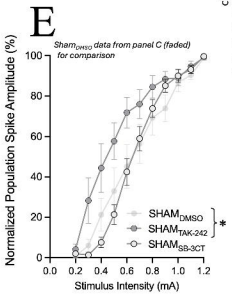
E
Sham DMSO data from panel C (faded) for comparison
Normalized Population Spike Amplitude (%)
Stimulus Intensity (mA)
SHAM DMSO
SHAM TAK-242
SHAM SB-3CT
*

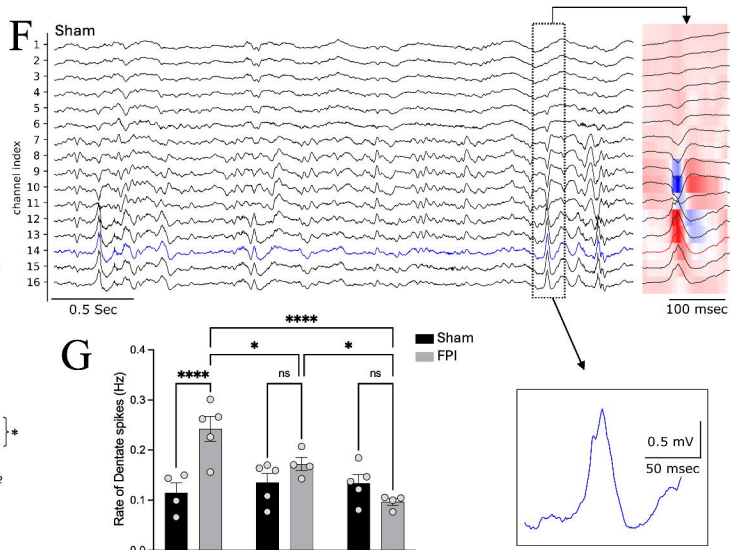
F
Sham
channel index
0.5 Sec
100 msec
0.5 mV
50 msec
G
Rate of Dentate spikes (Hz)
Sham
FPI
****
*
*
****
ns
ns
Vehicle
TAK-242
SB-3CT

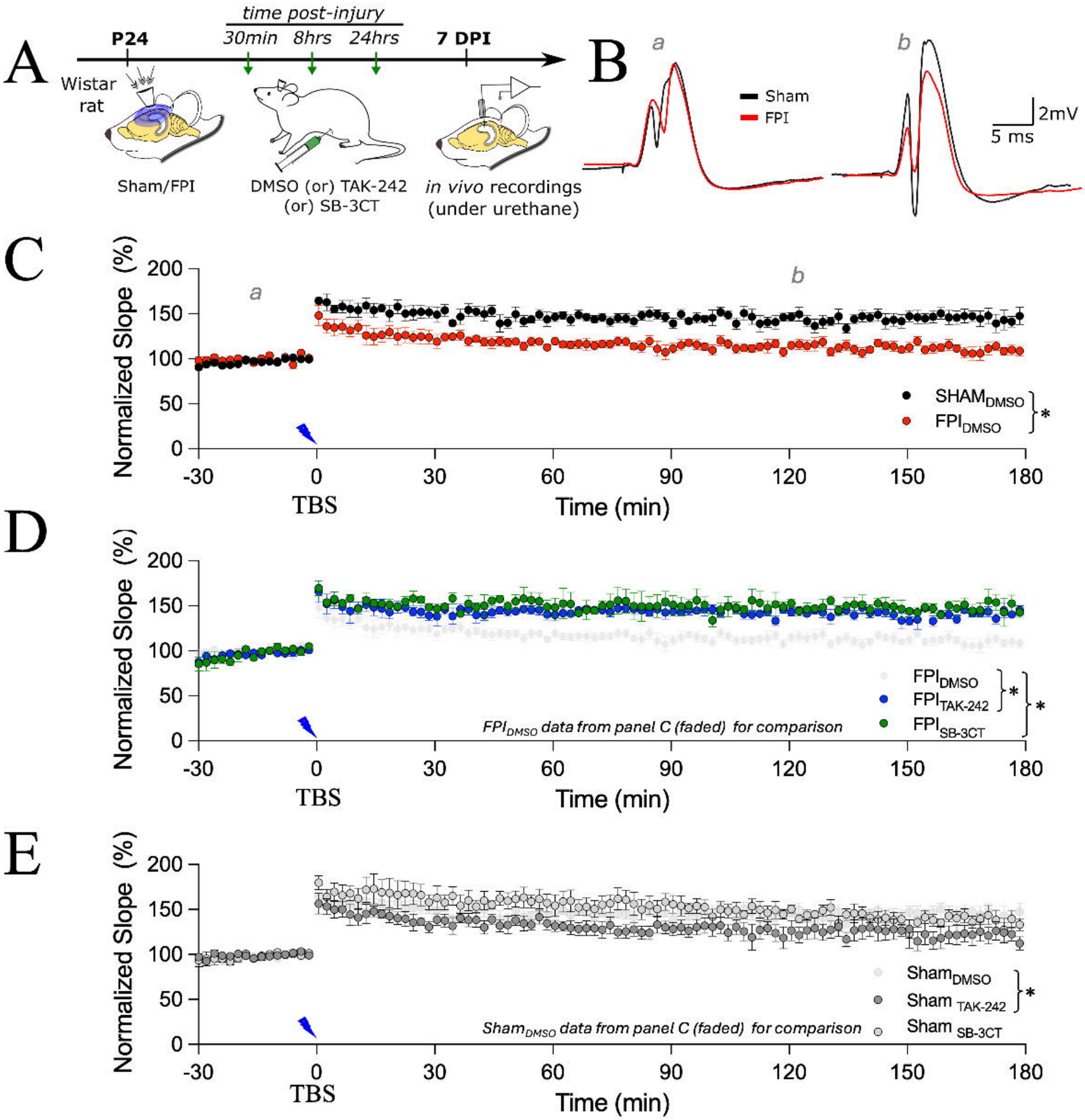
A
time post-injury
P24
30min
8hrs
24hrs
7 DPI
Wistar rat
Sham/FPI
DMSO (or) TAK-242 (or) SB-3CT
in vivo recordings (under urethane)
B
a
b
Sham
FPI
2mV
5 ms
C
Normalized Slope (%)
SHAM_DMSO
FPI_DMSO
TBS
Time (min)
D
FPI_DMSO
FPI_TAK-242
FPI_SB-3CT
FPI_DMSO data from panel C (faded) for comparison
E
Sham_DMSO
Sham TAK-242
Sham SB-3CT
Sham_DMSO data from panel C (faded) for comparison

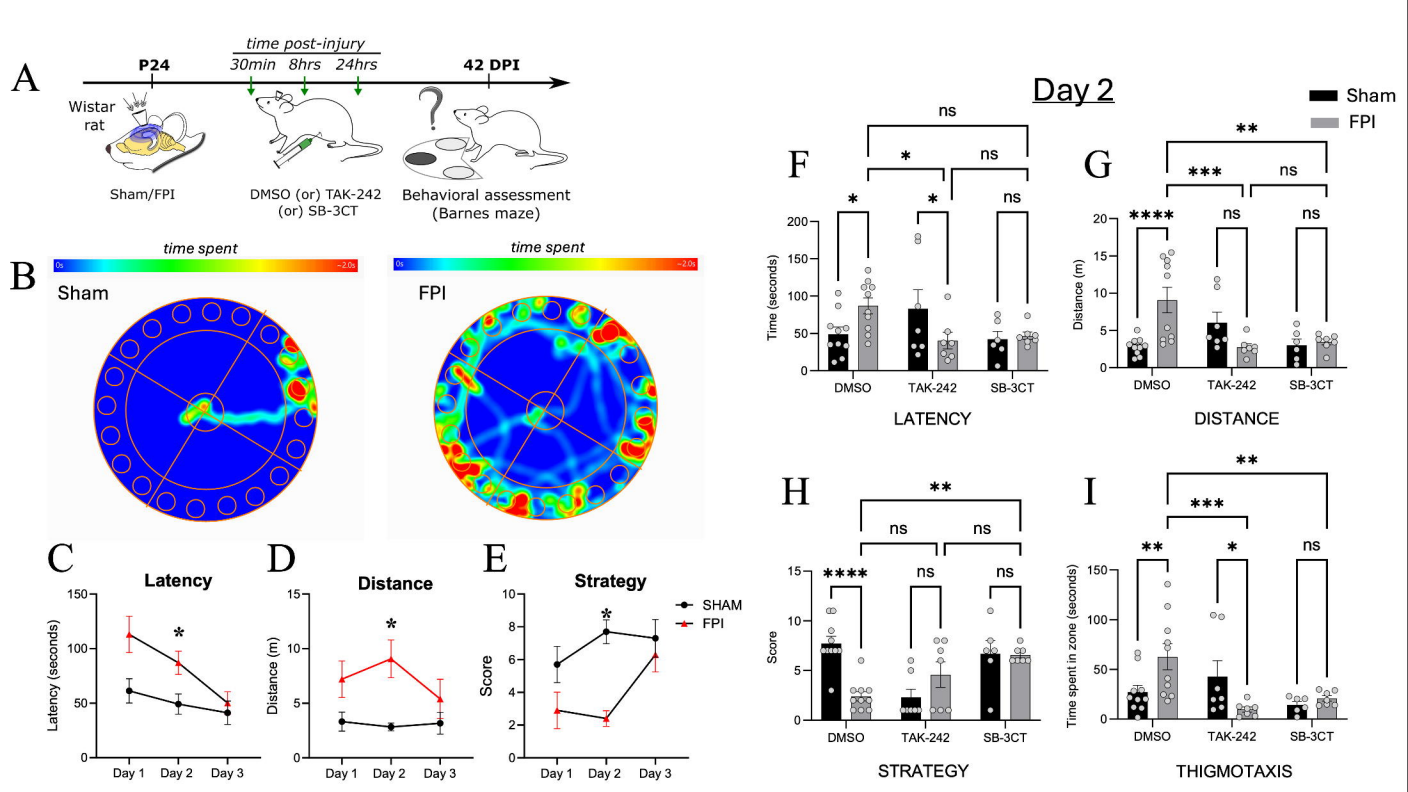
A
time post-injury
P24
30min
8hrs
24hrs
42 DPI
Wistar rat
Sham/FPI
DMSO (or) TAK-242 (or) SB-3CT
Behavioral assessment (Barnes maze)
B
time spent
Sham
FPI
C
Latency
Latency (seconds)
Day 1
Day 2
Day 3
D
Distance
Distance (m)
E
Strategy
Score
SHAM
FPI
Day 2
Sham
FPI
F
Time (seconds)
DMSO
TAK-242
SB-3CT
LATENCY
G
Distance (m)
DISTANCE
H
Score
STRATEGY
I
Time spent in zone (seconds)
THIGMOTAXIS
ns
*
**
***
****

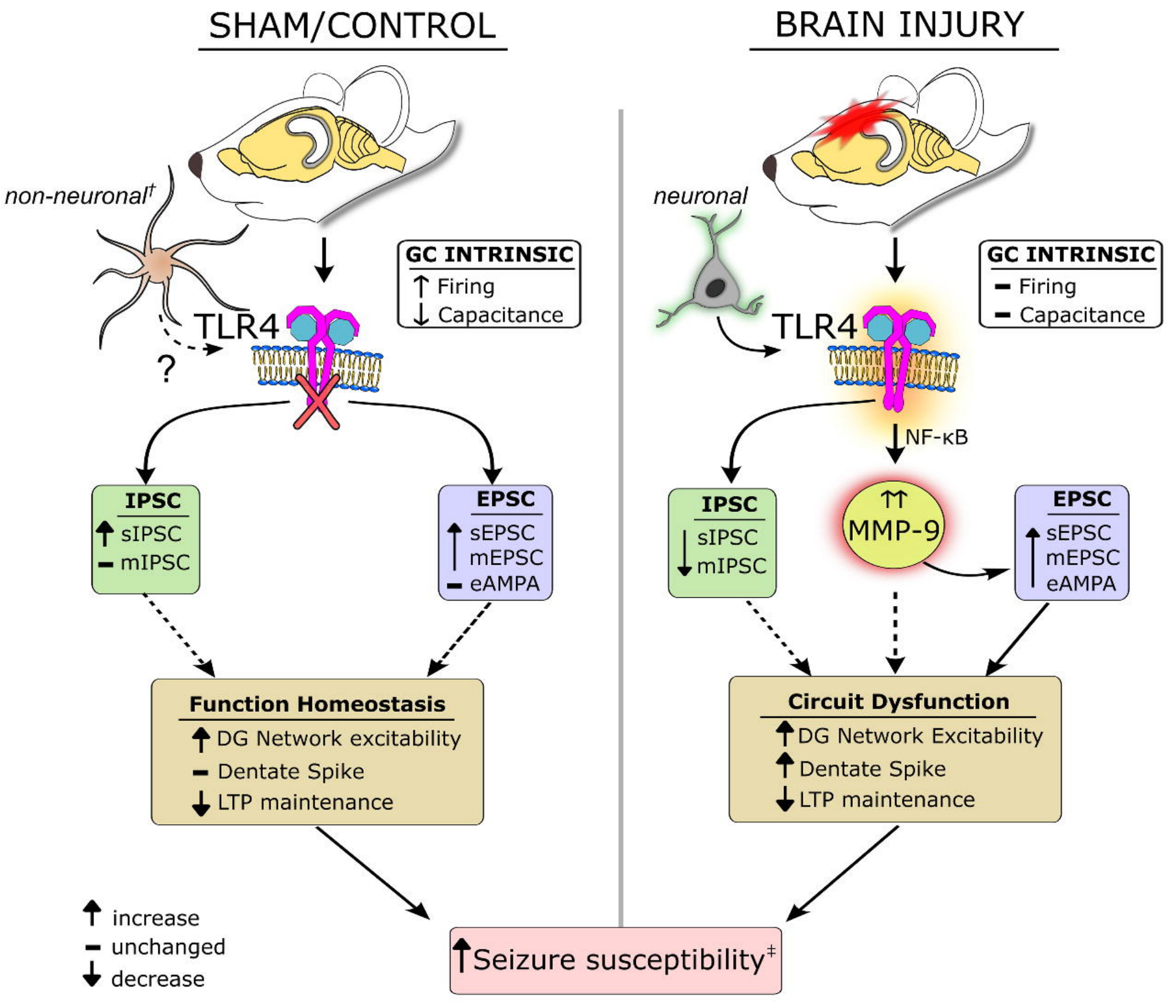
SHAM/CONTROL
BRAIN INJURY
non-neuronal†
neuronal
TLR4
?
GC INTRINSIC
↑ Firing
↓ Capacitance
GC INTRINSIC
– Firing
– Capacitance
NF-κB
IPSC
↑ sIPSC
– mIPSC
EPSC
↑ sEPSC
mEPSC
– eAMPA
IPSC
↓ sIPSC
mIPSC
↑↑
MMP-9
EPSC
↑ sEPSC
mEPSC
eAMPA
Function Homeostasis
↑ DG Network excitability
– Dentate Spike
↓ LTP maintenance
Circuit Dysfunction
↑ DG Network Excitability
↑ Dentate Spike
↓ LTP maintenance
↑ increase
– unchanged
↓ decrease
↑Seizure susceptibility‡